UNIVERSIDADE ESTADUAL PAULISTA

FACULDADE DE CIÊNCIAS AGRÁRIAS E VETERINÁRIAS

CÂMPUS JABOTICABAL

ALTERAÇÕES MORFOFISIOLÓGICAS E MOLECULARES EM CORPO LÚTEO BOVINO APÓS ADMINISTRAÇÃO DE DIFERENTES PROSTAGLANDINAS E DOSES NO METAESTRO E DIESTRO

Marina Anchieta Trevisoli

Médica Veterinária

2023

UNIVERSIDADE ESTADUAL PAULISTA

FACULDADE DE CIÊNCIAS AGRÁRIAS E VETERINÁRIAS

CÂMPUS JABOTICABAL

ALTERAÇÕES MORFOFISIOLÓGICAS E MOLECULARES EM CORPO LÚTEO BOVINO APÓS ADMINISTRAÇÃO DE DIFERENTES PROSTAGLANDINAS E DOSES NO METAESTRO E DIESTRO

Discente: Marina Anchieta Trevisoli

Orientadora: Profa. Dra. Lindsay Unno Gimenes

Coorientador: Prof. Dr. Juliano Coelho da Silveira

Dissertação apresentada à Faculdade de Ciências Agrárias e Veterinárias – Unesp, Câmpus de Jaboticabal, como parte das exigências para obtenção do título de Doutora em Medicina Veterinária (Área: Reprodução Animal).

2023

T814a

Trevisoli, Marina Anchieta

Alterações morfofisiológicas e moleculares em corpo lúteo bovino após administração de diferentes prostaglandinas e doses no metaestro e diestro / Marina Anchieta Trevisoli. -- Jaboticabal, 2023

74 p.

Dissertação (mestrado) - Universidade Estadual Paulista (Unesp), Faculdade de Ciências Agrárias e Veterinárias, Jaboticabal

Orientadora: Profa. Dra. Lindsay Unno Gimenes

Coorientador: Prof. Dr. Juliano Coelho da Silveira

1. Corpo lúteo. 2. miRNA. 3. PGF2. 4. Vias luteolíticas. I. Título.

Sistema de geração automática de fichas catalográficas da Unesp. Biblioteca da Faculdade de Ciências Agrárias e Veterinárias, Jaboticabal. Dados fornecidos pelo autor(a).

Essa ficha não pode ser modificada.

IMPACTO POTENCIAL DESTA PESQUISA

O impacto desta pesquisa consiste em determinar perfis morfo-funcionais e moleculares que ocorrem no corpo lúteo bovino após a administração de prostaglandinas em diferentes fases do ciclo. Essa contribuição é válida para direcionar projetos futuros que tenham como objetivo o estudo das vias luteolíticas, potencializando as biotecnologias reprodutivas.

POTENTIAL IMPACT OF THIS RESEARCH

The impact of this research consists in determining morpho-functional and molecular profiles that occur in the bovine corpus luteum after the administration of prostaglandins in different phases of the cycle. This contribution is valid for directing future projects that aim to study the luteolytic pathways, enhancing reproductive biotechnologies

UNIVERSIDADE ESTADUAL PAULISTA

Câmpus de Jaboticabal

CERTIFICADO DE APROVAÇÃO

TÍTULO DA DISSERTAÇÃO: ALTERAÇÕES MORFOLÓGICAS E MOLECULARES EM CORPO LÚTEO BOVINO APÓS ADMINISTRAÇÃO DE DIFERENTES PROSTAGLADINAS E DOSES NO METAESTRO E DIESTRO

AUTORA: MARINA ANCHIETA TREVISOLI
ORIENTADORA: LINDSAY UNNO GIMENES
COORIENTADOR: JULIANO COELHO DA SILVEIRA

Aprovada como parte das exigências para obtenção do Título de Mestra em Medicina Veterinária, área: Reprodução Animal pela Comissão Examinadora:

Profa. Dra. LINDSAY UNNO GIMENES (Participaçao Presencial)
Departamento de Patologia Reproducao e Saude Unica / FCAV UNESP Jaboticabal

Dra. ALESSANDRA BRIDI (Participaçao Presencial)
FMVZ/USP / Pirassununga/SP

Pesquisador Dr. FABIO MORATO MONTEIRO (Participaçao Presencial)
Instituto de Zootecnia / Sertãozinho/SP

Jaboticabal, 05 de maio de 2023

DADOS CURRICULARES DO AUTOR

MARINA ANCHIETA TREVISOLI – Nascida no dia 15 de março de 1997, em Rio Verde – GO; Filha de Francismar de Camargo Anchieta Trevisoli e Rogério Trevisoli; Formou-se em veterinária pela Universidade Estadual Paulista "Júlio de Mesquita Filho" – UNESP/FCAV – Câmpus Jaboticabal no dia 1 de fevereiro de 2019. Nessa mesma unidade realizou projeto de iniciação cientifica intitulada "Avaliação da Qualidade de Embriões Produzidos *in vitro* Obtidos de Vacas Nelores (*Bos indicus*) no Período Pós-Parto" sob orientação da Profa. Dra. Lindsay Unno Gimenes, tendo como entidade financiadora PIBIC/Reitoria/UNESP, durante o período de 01 de agosto de 2015 até 31 de julho de 2016. O título de Bacharel em Veterinário foi concedido pelo trabalho de conclusão de curso intitulado "Manejo reprodutivo de vacas no pós-parto da granja leiteira da Universidade de Illinois- UIUC" realizado na Universidade de Illinois – UIUC no ano de 2018. Em junho de 2020 ingressou no programa de mestrado em medicina veterinária, área de reprodução animal, pela UNESP - Universidade Estadual Paulista "Júlio de Mesquita Filho", Faculdade de Ciências Agrárias e Veterinárias - Câmpus de Jaboticabal, finalizando em 01 de julho de 2023, sendo bolsista da Coordenação de Aperfeiçoamento de Pessoal de Nível Superior (CAPES).

“Até aqui nos ajudou o Senhor”

I Samuel 7:12

AGRADECIMENTOS

Agradeço primeiramente a minha família, que por todos esses anos que me dediquei a academia sempre me apoiaram e acreditaram em mim mesmo quando eu mesma desacreditei. Eternamente grata, Rogério, Francismar, Talitha e Priscila Trevisoli.

Gostaria me especial á Profa. Dra. Lindsay Unno Gimenes que me acompanha em toda minha trajetória na universidade, desde estágios supervisionados, iniciação cientifica, coordenação de grupos de estudos e orientadora de trabalho de conclusão de curso e por fim, no mestrado. Imensa gratidão pelos ensinamentos tanto científicos como pessoal.

Um agradecimento aos amigos pelo apoio durante todos os momentos que em que precisei de ajuda. E aos colegas de pós-graduação que ajudaram tanto na execução do projeto, como também como ombro amigo.

Por fim, agradecer a Deus por todas as oportunidades que me foram oferecidas e por todo apoio que me proporcionou em todas as etapas da minha vida.

“O presente trabalho foi realizado com apoio da Coordenação de Aperfeiçoamento de Pessoal de Nível Superior - Brasil (CAPES) - Código de Financiamento 001”.

SUMÁRIO

Página

CERTIFICADO DA COMISSÃO DE ÉTICA NO USO DE ANIMAIS

UNIVERSIDADE ESTADUAL PAULISTA
"JÚLIO DE MESQUITA FILHO"
Câmpus de Jaboticabal

CEUA – COMISSÃO DE ÉTICA NO USO DE ANIMAIS

CERTIFICADO

Certificamos que o projeto de pesquisa intitulado **"Avaliação da eficiência luteolítica de diferentes doses de cloprostenol sódico e dinoprost trometamina administradas nos dias 4 e 11 do ciclo estral de vacas de corte"**, protocolo nº 006001/18, sob a responsabilidade da Prof.ª Dr.ª Lindsay Unno Gimenes, que envolve a produção, manutenção e/ou utilização de animais pertencentes ao Filo Chordata, subfilo Vertebrata (exceto o homem), para fins de pesquisa científica (ou ensino) - encontra-se de acordo com os preceitos da lei nº 11.794, de 08 de outubro de 2008, no decreto 6.899, de 15 de julho de 2009, e com as normas editadas pelo Conselho Nacional de Controle de Experimentação Animal (CONCEA), e foi aprovado pela COMISSÃO DE ÉTICA NO USO DE ANIMAIS (CEUA), da FACULDADE DE CIÊNCIAS AGRÁRIAS E VETERINÁRIAS, UNESP - CÂMPUS DE JABOTICABAL-SP, em reunião ordinária de 10 de maio de 2018.

Vigência do Projeto	25/05/2018 a 20/12/2018
Espécie / Linhagem	Bovina / Nelore ou Mestiça
Nº de animais	124
Peso / Idade	Peso médio 400 Kg / Acima de 18 meses
Sexo	Fêmea
Origem	Guatapará – SP

Jaboticabal, 10 de maio de 2018.

Fabiana Pilarski

Profª Drª Fabiana Pilarski
Coordenadora – CEUA

Faculdade de Ciências Agrárias e Veterinárias
Via de Acesso Prof. Paulo Donato Castellane, s/n - 14884-900 - Jaboticabal - SP - Brasil
tel 16 3209 2600 fax 3202 4275 www.fcav.unesp.br

ALTERAÇÕES MORFOFISIOLÓGICAS E MOLECULARES EM CORPO LÚTEO BOVINO APÓS ADMINISTRAÇÃO DE DIFERENTES PROSTAGLANDINAS E DOSES NO METAESTRO E DIESTRO

RESUMO – O objetivo do presente estudo foi investigar os processos relacionados à administração de diferentes prostaglandinas (cloprostenol sódico - CS e dinoprost trometamina - DT) utilizando 100% e 50% da dose recomendada, durante metaestro e diestro (4 e 11 dias após ovulação (D0), respectivamente). Foram analisadas as seguintes características: dinâmica luteal, vascularização do CL, quantificação de pixels na perfusão sanguínea do CL e dosagem sérica de progesterona (P4) (Exp.1) e morfometria das células luteais, valor numérico de pixels (NVP) e heterogeneidade associada ao CL e imunomarcação da caspase-3, dosagem de P4 e expressão de microRNA (miRNA) (Exp.2). Em Exp. 1, 44 fêmeas tiveram ovulação sincronizada e receberam os seguintes tratamentos: D4 (CS50% n= 5; CS100% n= 5; DT50% n= 5; DT100% n= 5) e D11 (CS50% n= 7; CS100% n= 5; DT50% n= 6; DT100% n= 6). Em Exp. 2, foram sincronizadas 23 fêmeas, alocadas nos tratamentos: D4 (CS 50%, n=3; CS 100%, n=3; DT 50%, n=3; DT 100%, n=3) e D11 (CS 50 %, n=3; CS 100%, n=3; DT 50%, n=3; DT 100%, n=2) e foram abatidos dois dias depois. Os dados foram analisados por ANOVA em arranjo fatorial (2x2, no Exp. 1 e Exp. 2) com medidas repetidas ao longo do tempo (exceto morfometria e imunomarcação) e teste de Tukey, com significância < 5%. A análise do miRNA foi descritiva. No metaestro, houve redução inicial de P4, independente da droga utilizada e da dose utilizada, retornando sua capacidade esteroidogênica após 96h (Exp.1). Quando utilizado 100%, houve declínio de P4 e redução da perfusão sanguínea do CL. Quando foram utilizados 50% da dose e DT, observou-se maior redução na área de pequenas células luteais, enquanto o tratamento DT50% apresentou maior heterogeneidade. CS100% teve maior redução de P4 (Exp.2), maior NVP, indicando processo luteolítico. Na fase de diestro, tanto 50% quanto 100% da dose de ambas as PGF2α diminuíram o nível sérico de P4, a vascularização, a perfusão sanguínea e o tamanho do CL (Exp.1). DT e dose de 100% alcançaram maior redução de células luteais grandes. O tratamento DT100% apresentou menor NVP, enquanto CS100% apresentou maior heterogeneidade. Foi possível identificar 18 miRNAs exclusivos no metaestro, nenhum no diestro e 5 em comum quando utilizada 50% da dose, independente da PGFα. Com 100% da dose, nenhum foi encontrado no metaestro, 8 miRNAs no diestro e 17 miRNAs em comum. A administração de luteolíticos no D4 foi sugestiva de luteólise parcial quando utilizada 100% da dose. A administração no D11 foi eficiente na indução da luteólise completa, utilizando 50% ou 100% da dose recomendada, independente do medicamento.

Palavras-chave: corpo lúteo, miRNA, PGF2α, vias luteolíticas

MORPHOPHYSIOLOGICAL AND MOLECULAR CHANGES IN BOVINE CORPUS LUTEUM AFTER ADMINISTRATION OF DIFFERENT PROSTAGLANDINS AND DOSES IN METAESTRUS AND DIESTRUS

ABSTRACT - The objective of the present study was to investigate the processes related to the administration of different prostaglandins (sodium cloprostenol - CS and dinoprost tromethamine - DT) using 100% and 50% of the recommended dose, during metestrus and diestrus (4 and 11 days after ovulation (D0), respectively). The following features were analyzed: luteal dynamics, CL vascularization, quantification of pixels in CL blood perfusion and serum progesterone (P4) measurement (Exp.1) and luteal cell morphometry, numerical value of pixels (NVP) and heterogeneity associated to CL caspase-3 immunostaining, P4 and microRNA (miRNA) expression (Exp.2). In Exp. 1, 44 females had synchronized ovulation and received the following treatments: D4 (CS50% n= 5; CS100% n= 5; DT50% n= 5; DT100% n= 5) and D11 (CS50% n= 7; CS100% n= 5; DT50% n= 6; DT100% n= 6). In Exp. 2, 23 females were synchronized, allocated to treatments: D4 (CS 50%, n=3; CS 100%, n=3; DT 50%, n=3; DT 100%, n=3) and D11 (CS 50%, n=3; CS 100%, n=3; DT 50%, n=3; DT 100%, n=2) and were slaughtered two days later. Data were analyzed by ANOVA in a factorial arrangement (2x2, in Exp. 1 and Exp. 2) with repeated measurements over time (except for morphometry and immunostaining) and Tukey's test, with significance at < 5%. The miRNA analysis was descriptive. At metestrus, there was an initial reduction in P4, regardless of the drug used and dose used, returning its steroidogenic capacity after 96h (Exp.1). When 100% was used, there was a decline in P4 and a reduction in CL blood perfusion. When 50% of the dose and DT were used, a greater reduction in the area of small luteal cells was observed, while the 50%DT treatment had a greater heterogeneity. CS100% had a greater reduction in P4 (Exp.2), higher NVP, indicating a luteolytic process. In the diestrus phase, both 50% and 100% of the dose of both PGF2α decreased the serum level of P4, vascularization, blood perfusion, and CL size (Exp.1). DT and 100% dose achieved greater reduction of large luteal cells. The DT100% treatment had lower NVP, while CS100% in higher heterogeneity. It was possible to identify 18 unique miRNAs in metestrus, none in diestrus and 5 in common when 50% of the dose was used, regardless of PGFα. With 100% of the dose, none were found in metestrus, 8 miRNAs in diestrus and 17 miRNAs in common. The administration of luteolytics in D4 was suggestive of partial luteolysis when 100% of the dose was used. Administration on D11 was efficient in inducing complete luteolysis, using 50% or 100% of the recommended dose, regardless of the drug.

Keywords: corpus luteum, luteolytic pathways, miRNA, PGF2α

LISTA DE TABELAS

Página

LISTA DE FIGURAS

Página

CAPÍTULO 1 – Considerações Gerais

1. INTRODUÇÃO

A produtividade do rebanho bovino é altamente relacionada com a eficácia na reprodução dos animais, fazendo com que os estudos envolvendo fisiologia básica seja fundamental para posterior aplicação das biotécnicas da reprodução. O ciclo reprodutivo da fêmea bovina tem, em média, duração de 21 dias e é classificada em fases baseadas nas oscilações hormonais. Tal ciclo pode ser dividido em fase folicular e luteal, sendo que na primeira o hormônio predominante é o estradiol (E2) e na segunda, a progesterona (P4) (HAFEZ, B.; HAFEZ, 2004). Para se iniciar um novo ciclo é necessário que ocorra a luteólise, que fisiologicamente ocorre por volta do dia 17 após a ovulação (SARTORI et al., 2004).

A regressão do corpo lúteo (CL) ocorre por meio da ação da prostaglandina F-2alfa (PGF2α) e apresenta duas fases: a luteólise funcional e, em seguida, a estrutural. A funcional é caracterizada pelo abrupto declínio nas concentrações séricas de P4 durante as primeiras 8 a 12 horas após a admnistração da PGF2α. Já a luteólise estrutural é o processo de diminuição de tamanho até regressão total do CL formando o *corpus albicans* (MCCRACKEN; CUSTER; LAMSA, 1999; STOCCO; TELLERIA; GIBORI, 2007).

Os análogos da PGF2α são mundialmente difundidos com a função de mimetizar a ação na luteólise. Comercialmente no Brasil existem três princípios ativos disponíveis: o dinoprost trometamina (DT), cloprostenol sódico e d-cloprostenol, sendo os dois últimos compostos sintéticos e o primeiro, um análogo natural. Estudos comparando a eficiência dos fármacos foram realizados e, apesar de alguns resultados indicarem diferença quanto à eficiência de regressão luteal, outros demonstraram similaridade quanto à taxa de concepção ao final de protocolos de sincronização de estro (ETHERINGTON; KELTON; ADAMS, 1994; PURSLEY et al., 2012; STEVENSON; PHATAK, 2010). Com o objetivo de otimização dos protocolos, também foi testada a redução de doses, obtendo-se resultados eficazes utilizando até 50% da dose recomendada, porém quando utilizada 25% da dose recomendada se constatou um breve declínio da P4 com posterior aumento, causando o que se

conhece como luteólise parcial, na qual não ocorre a cascata necessária para a regressão total do CL (NASCIMENTO et al., 2014b; TREVISOL et al., 2015).

No fim do processo da luteólise estrutural, ocorre a apoptose das células que é um processo de morte celular, degeneração de DNA e posterior remodelamento da matriz (MARTIN, 2014). Esse processo pode ocorre por meio de duas vias, extrínseca ou intrínseca e o seu desencadeamento promove ativação de cascatas de caspases que serão responsáveis por promover a total desintegração celular. A mais comumente estudada é a caspase-3, sendo avaliada sua presença e expressão de RNAm relacionados à luteólise (GRIVICICH; REGNER; DA ROCHA, 2007; HOJO et al., 2016; PELUFFO et al., 2006).

Os avanços da biologia molecular estão sendo difundidos na reprodução animal, a fim de elucidar o complexo processo da luteólise. Recentemente são crescentes os estudos utilizando mircroRNAs (miRNAs), que são pequenas moléculas que atuam na regulação da tradução das proteínas, para compreensão das vias que são ativas ou não durante a regressão do CL de ruminantes (GECAJ et al., 2017; HOSSAIN et al., 2012; MCBRIDE et al., 2012). Dessa forma, neste capítulo iremos abordar as modificações morfofisiológicas e moleculares que ocorrem durante o processo da luteólise.

2. REVISÃO BIBLIOGRÁFICA

2.1. Ciclo estral bovino

O ciclo estral dos bovinos possui, em média, 21 dias de duração e pode ser dividido em duas fases baseado nos hormônios que dominam cada momento. São elas, a fase estrogênica que precede a ovulação e a fase progesterônica, que se inicia após a ovulação e formação do corpo lúteo (CL) e se encerra com a regressão do CL, o que fisiologicamente ocorre por volta de 17 a 18 dias após a ovulação (SARTORI et al., 2004). A luteólise é necessária para que possa ocorrer um novo pico de LH e, assim, nova ovulação nos casos onde não ocorreu o reconhecimento embrionário (MCCRACKEN; CUSTER; LAMSA, 1999).

Dentro da fase luteal, podemos observar duas distintas fases, o metaestro que é o momento inicial, onde ocorre a transformação das células foliculares em células luteínicas e todo o remodelamento para início da produção de P4, esta fase dura cerca

de 2 a 3 dias. A fase de manutenção do CL é classificada como diestro, que se inicia quando o CL já está em pleno funcionamento e se finda com a sua regressão (revisado por Myamoto et al. (2009).

2.2. Formação do CL

O CL é considerado como um órgão endócrino transitório, ou seja, é responsável pela síntese de P4 durante o período onde o endométrio se prepara para a implantação e manutenção de uma possível gestação, regredindo caso não ocorra a implantação do embrião (GIRSH et al., 1996; MILVAE, 2000; WILTBANK, 1994). Após a ovulação se inicia o processo de remodelamento de células na cavidade formada pela expulsão do oócito do folículo dominante, resultando em um corpo hemorrágico. As células da granulosa e teca iniciam um processo de hiperplasia e hipertrofia, e também ocorre a proliferação de novos vasos sanguíneos, que são responsáveis pelo aumento de fluxo sanguíneo ao longo do desenvolvimento do CL (DAMBER et al., 1987).

A composição celular do CL é bem heterogênea, sendo composta por células luteínicas esteroidoigênicas grandes (LLC- *Large Luteal Cells*) e pequenas (SLC – *Small Luteal Cells*) e são formadas a partir da transformação das células da granulosa e teca, respectivamente (ALILA; HANSEL, 1984), além de células não-esteroidoigênicas, como células endoteliais, fibroblastos e células do sistema imune (O'SHEA; RODGERS; D'OCCHIO, 1989). As LLC medem mais que 20μm e são responsáveis pela maior parte da produção de P4 do CL. Já as SLC são caracterizadas por medirem menos de 20μm e possuírem maior quantidade de receptores para o LH, fazendo com que elas sejam mais responsivas à atuação deste, diferente das LLC que apesar de apresentarem receptores de LH não respondem muito à estimulação do mesmo (FITZ et al., 1982).

A vasta rede de capilares formados pelas células endoteliais representa mais de 50% do total do número de células presentes em todo o CL, fazendo com que a maioria das células esteroidoigênicas tenha um íntimo contato com esses capilares (O'SHEA; RODGERS; D'OCCHIO, 1989). A angiogênese e vascularização se desenvolvem rapidamente a partir da atuação de fatores vasoativos produzidos pelo próprio CL, sendo os principais o fator de crescimento endotelial vascular (VEGF –

vascular endotelial growth factor), o fator de crescimento fibroblástico (FGF - *fibroblast growth factor*), as angiopoetinas (ANPT) 1 e 2 (revisado por MIYAMOTO; SHIRASUNA; SASAHARA, 2009; SCHAMS et al., 2003), a endotelina-1 (ENDT1) e angiotensina II (Ang II) (revisado por TREVISOL et al., 2015).

O VEGF e FGF tem uma importante ação mitogênica nas células endoteliais, induzindo a migração e proliferação das mesmas, além do controle da permeabilidade dos vasos sanguíneos (NASH et al., 2006). As ANTPs são necessárias para o desenvolvimento do CL, tendo em vista que a ANPT-1 tem a função de estabilizar os vasos sanguíneos, já a ANTP-2 os desestabiliza. Com isso, a relação entre ANTP-1/ANTP-2 é crucial para o desenvolvimento e manutenção dos vasos sanguíneos durante toda a fase luteínica (SCHAMS et al., 2003). A Ang II tem sua maior atuação quando a atividade de angiogênese está alta, ou seja, no início da formação do CL (KOBAYASHI et al., 2001). Contudo experimentos na fase do diestro, com a aplicação de PGF2α demonstrou um aumento de Ang II, provocando a inibição da secreção de progesterona (HAYASHI; MIYAMOTO, 1999). A ENDT-1 tem alto poder vasoconstritor e está altamente expressa na formação do CL e na fase de regressão. Sua modulação ocorre devido à formação de dois receptores, o ETR-A e o ETR-B. O ETR-A está presente em todo o ciclo e tem função antiapoptótica, já o ETR-B aumenta na fase luteolítica, auxiliando nos processos apoptóticos (BERISHA; SCHAMS; MIYAMOTO, 2002; FILIPPATOS et al., 2001).

Com toda a rede vascular formada, as células esteroidoigênicas podem, por fim, exercer a total capacidade de produção de P4. Essa fase de pleno funcionamento e manutenção do CL, corresponde à fase de diestro (revisado por (MIYAMOTO; SHIRASUNA; SASAHARA, 2009). Todo esse processo de vascularização inicial, manutenção e regressão dos capilares do CL pode ser observado por exames ultrassonográficos em modo Doppler (PUGLIESI; NAVES, 2017). Acosta e colaboradores (2002) utilizaram essas imagens coloridas onde é possível avaliar as alterações do fluxo sanguíneo do CL. Em vacas leiteiras foi possível obter uma correção positiva entre o fluxo sanguíneo avaliado por meio do Doppler com a secreção de P4 (KAYA et al., 2017).

2.3. Luteólise

A lise do CL é marcada por um complexo processo em que todo o tecido formado após a ovulação sofre mudanças de remodelamento, findando na substituição de um órgão endócrino em tecido conjuntivo, conhecido como *corpus albicans* (STOCCO; TELLERIA; GIBORI, 2007). A PGF2α é reconhecida como hormônio luteolítico natural de várias espécies mamíferas (WAITE; HOLTAN; STORMSHAK, 2005). Produzida pelo endométrio e transportada pela circulação útero-ovárica, esta prostaglandina é responsável pelo desencadeamento das alterações no CL, causando a luteólise (CUNNINGHAM,2004).

A luteólise pode ser estratificada em duas fases: a luteólise funcional, que corresponde ao declínio da secreção de P4 pelas células luteínicas e a luteólise estrutural que se inicia após o declínio de progesterona e é determinada pela apoptose celular do CL (STOCCO; TELLERIA; GIBORI, 2007). Ginther e colaboradores (2010) identificaram a luteólise funcional de fêmeas bovinas em três fases. Essa divisão está relacionada às flutuações sofridas pela P4 em um período de 24 horas: a pré-luteolítica corresponde ao período anterior ao início da redução de P4, a luteolítica consiste no grande declínio das concentrações de P4 e a pós-luteolítica é quando os níveis séricos se encontram abaixo de 1ng/mL.

O mecanismo de liberação da PGF2α necessária para causar a luteólise fisiológica em bovinos se inicia por meio de pulsos (4 a 7 pulsos) de curta duração (entre 3 e 6 horas) durante 2 a 3 dias (GINTHER et al., 2007, 2010; KINDHAL, H.; LINDELL, J. O.; EDQVIST, 1981). A pulsatilidade da secreção da PGF2α foi observada durante os três períodos distintos por meio da mensuração do seu metabólito em bovinos (GINTHER et al., 2007). Nesse estudo, pode-se observar que durante o período pré-luteolítico os picos ocorrem em baixos níveis com um leve declínio de P4; contudo, foi observado um efeito rebote. Durante o período luteolítico os picos são de maior pico e amplitude, não permitindo ocorrer o efeito rebote de aumento de P4, desencadeando assim uma cascata luteolítica envolvendo uma série de reguladores das funções do CL, como citocinas, fatores de crescimento e alteração do fluxo sanguíneo.

A PGF2α se liga aos receptores localizados nas membranas das células luteínicas (em maior quantidade nas LLC, onde há maior presença de receptores

(NISWENDER et al., 2000a), os quais são mediados por proteína G. A ativação desse receptor irá promover a produção de inusitol trifosfato (IP3) e diaciglicerol (DAG), por meio de uma reação mediada pela ação da fosfolipase C (CHEN et al., 1998; DAVIS; RUEDA, 2002). Com a ativação da fosfolipase C, há indícios que ocorre a ativação da fosfolipase D, produzindo ácido fosfatídico que, em contato com o DAG, irá ativar a cascata sinalizadora da MAP quinase, outra importante via para a continuação do processo de luteólise (TAI et al., 2001).

O primeiro efeito observado após o início da ação da PGF2α é o decréscimo do fluxo sanguíneo, afetando diretamente a secreção de P4 (MIYAMOTO; SHIRASUNA; SASAHARA, 2009). *A priori*, se observa aumento de fluxo na área luteal periférica devido à ação do NO, sugerindo que o aumento do fluxo sanguíneo após a ação da PGF2α é um dos sinais de ativação da cascata de luteólise (ACOSTA et al., 2002a; MIYAMOTO; SHIRASUNA; SASAHARA, 2009). Outra ação inicial da prostaglandina é a supressão da produção dos fatores de crescimento no CL, como o VEGF. Substâncias vasoativas como a EDN1, Ang II, e a PGF2α de origem luteal irão causar uma severa vasoconstrição, acelerando o processo (revisado por MIYAMOTO; SHIRASUNA; SASAHARA, 2009). Como o processo em que a PGF2α afeta a produção da P4 ainda não foi totalmente elucidado, estudos indicaram que a PGF2α exógena causa redução no RNAm de fatores esteroidoigênicos, como a proteína reguladora de progesterona (Star), da mesma forma que reduzem os fatores angiogênicos. Em contrapartida, sua ação aumenta a produção de fatores relacionados à síntese de prostaglandinas, como a COX-2 (SHIRASUNA et al., 2010).

Outra via ativada após ocorrer a ligação da PGF2α com seu receptor é o aumento da proteína quinase C que, consequentemente, vai desencadear aumento de Ca^{2+} intracelular (NISWENDER et al., 2000a). Esse aumento de influxo de Ca^{2+} intracelular está altamente relacionado ao desencadeamento do processo de apoptose e morte celular, que correspondem com a próxima fase do processo de regressão do CL, a luteólise estrutural. A apoptose, é conhecida como o processo de morte celular, ou seja, um conjunto de alterações morfológicas como diminuição do tamanho, fragmentação do DNA e alterações das membranas, que por fim geralmente são fagocitadas por células especializadas, como por exemplo, os macrófagos (CAROU et al., 2015). Os capilares sanguíneos são os primeiros a sofrerem o

processo de degeneração, causando a protrusão das células endoteliais em direção ao lúmen, causando sua fragmentação e completa desintegração (KNICKERBOCKER; WILTBANK; NISWENDER, 1988). As alterações de diâmetro do CL podem ser observadas por imagens ultrassonográficas a partir de 12 horas após o início da liberação da PGF2α (ACOSTA et al., 2002b)

O processo de apoptose possui duas principais vias de ativação: extrínseca (mediada por receptores) ou intrínseca (mediada por via mitocondrial, intracelular). A via intrínseca é iniciada a partir de uma situação de estresse, como por exemplo hipoxia sofrida pela célula, alterando a atividade mitocondrial levando o citocromo C, a ligar-se a fatores apoptóticos ativadores de proteases e procaspase-9, levando à ativação da caspase-9. Já a sinalização da via extrínseca ocorre por meio da ativação dos chamados “receptores de morte” o Fas ligand e Fator de necrose tumoral (TNF – *tumoral necrose factor*). Esses receptores irão fazer a ativação da caspase-8. As caspases são pertencentes a uma família de cisteina-proteases, que estão presentes nas células de forma inativada (TIZARD, 2014). Os fins de ambas as vias apoptóticas levam à ativação das caspases efetoras, que são as caspases-3, 6 e 7 (GRIVICICH; REGNER; DA ROCHA, 2007; STOCCO; TELLERIA; GIBORI, 2007).

A participação da caspase-3 na reprodução foi observada *in vitro* em células luteais de camundongos (CARAMBULA et al., 2002), demonstrando que essa molécula teve relação positiva no processo de apoptose, sendo observada nenhuma ou pouca expressão em animais que não apresentaram processos apoptóticos. Em bovinos, a participação das caspases foi demonstrada no CL por Nishimura e colaboradores (2008), resultando em maior atividade da enzima da caspase-3 quando colocadas sob baixa tensão de oxigênio, comparada com células em alta tensão, confirmando a participação da caspase-3 no processo apoptótico do CL. Yadav et al (2005), por meio de PCR em Tempo Real (qPCR), demonstraram aumento de mRNA da caspase-3 durante a luteólise induzida em ovinos por meio de PGF2α exógena, com isso podemos ressaltar a caspase 3 como um importante marcador luteolítico. Durante o processo de apoptose também ocorre um alto influxo de células imunes, como macrófagos e leucócitos que irão promover respostas inflamatórias e, assim, aumento de fatores quimiotáticos (MURDOCH, 1987). MiRNAs com funções regulatórias de recrutamento de células imunes foram encontradas em CL de

ruminantes durante a fase de diestro e regressão luteal, demonstrando a possível atuação dessas moléculas controlando o processo luteólitico (GECAJ et al., 2017; HOSSAIN et al., 2009; MCBRIDE et al., 2012).

2.4. Indução Exógena da Luteólise

Com o maior conhecimento sobre a ação fisiológica da PGF2α no processo de regressão luteal, pesquisadores iniciaram estudos usando a PGF2α como ferramenta para biotecnologias, possibilitando o desenvolvimento de protocolos de sincronização de estro (PURSLEY; MEE; WILTBANK, 1995). Entre as PGF2α comumente utilizadas, o análogo natural é o dinoprost trometamina (DT), possuindo uma meia-vida curta (7 a 8 minutos) devido ao seu alto metabolismo (KINDHAL; LINDELL, ; EDQVIST, 1981), sendo sua dose recomendada maior (25mg) comparada aos fármacos sintéticos. O análogo sintético mais utilizado é o cloprostenol sódico (CS) que, ao contrário do natural, tem meia-vida longa (aproximadamente 3 horas, (REEVES, 1978), possibilitando ação mais duradoura no organismo (BOURNE et al., 1980), com menor dose (500µg).

O interesse em ajustar os protocolos foi constante, como a alteração da via de administração, redução da dose utilizada e também qual seria o composto utilizado. Colazo e colaboradores (2002) analisaram o uso de cloprostenol sódico utilizando a dose recomendada pelo fabricante, comparando as vias de administração intramuscular (IM) e via subcutânea (SC). Também foi comparada com a via intravenosa (IV) por Stevens et al. (1995) e com a via submucosa intravulvar (IVSM) por Meira et al (2006), contudo ambos não tiveram diferença na taxa de luteólise quando comparada com a administração IM.

Com as vias de administração compreendidas, manipulações da dosagem utilizada para provocar a luteólise foram testadas. Comparando a via IVSM e IM quando se utilizou dose reduzida de CS, as taxas de prenhez não diferiram (CHACUR et al., 2010; GIOSO et al., 2005; MEIRA et al., 2006). No estudo de Meira e colaboradores (2016), quando se comparou a utilização do dobro da dose com 50% da dose recomendada em vacas Nelore, não se observou diferença na regressão do CL quando utilizado no diestro. Contudo, quando foram realizados estudos utilizando 25% da dose recomendada, apenas ocorreu luteólise parcial (GRANADOS-

VILLARREAL et al., 2017; MEIRA et al., 2006; TREVISOL et al., 2015). Este resultado também foi encontrando por Ginther et al (2009) quando trataram novilhas holandesas pelas vias de administração IV e intrauterina com subdosagem de prostaglandinas.

O termo “luteólise parcial” foi primeiramente utilizado por Stellflug e colaboradores (1977), quando se observou a dinâmica das concentrações de progesterona com aplicações de diferentes doses de PGF2α. Os animais que após os tratamentos não permaneceram com níveis séricos abaixo de 1,0 ng/mL, não tiveram a regressão total do CL. Resultados como este foram encontrados quando a administração das prostaglandinas foi realizada em fases diferentes do ciclo estral. Quando administrada no metaestro, a função luteolítica do fármaco não foi observada (SENGER, 2003). Nascimento et al (2014) demonstraram essa mesma refratariedade em vacas leiteiras aplicando duas doses de PGF2α no 5 dia após ovulação.

A refratariedade do CL à PGF2α no metaestro não se dá pela ausência de receptores de PGF2α (PGFR), pois a expressão de RNAm de PGFR se mantém durante toda a vida do CL (TSAI; WILTBANK, 1998). Shirashuna e colaboradores (2012) também obtiveram resultados onde foi comprovada a presença desses receptores no início do ciclo estral, contudo, observaram aumento do RNAm com o avançar do ciclo estral. Pesquisadores associaram essa refratariedade à presença em maior quantidade da enzima catalizadora de PGF2α (15-hydroxyprostaglandina dehydrogenase - PGDH) no início do ciclo estral (MIYAMOTO; SHIRASUNA; SASAHARA, 2009), ressaltando ainda mais a complexidade e cascata de eventos não totalmente elucidados a respeito do processo de luteólise do CL.

Quanto aos análogos da PGF2α, o estudo demonstrou diferenças nos quais o análogo natural, DT, teve uma resposta mais eficiente em protocolos de transferência de embriões (DONALDSON, 1984). Contudo o uso do fármaco sintético CS demonstrou melhores resultados na taxa de prenhez após o uso na sincronização do ciclo estral (PURSLEY et al., 2012; STEVENSON; PHATAK, 2010). Em cultivo *in vitro* de células luteais os compostos sintéticos promoveram maior influxo de cálcio intracelular, apoptose e contratilidade da artéria ovariana (KORZEKWA et al., 2014). Entretanto, outros pesquisadores encontraram resultados similares com a indução de estro, taxa de concepção e taxa de serviço por concepção quando compararam os análogos DT e CS (DONALDSON, 1984; ETHERINGTON; KELTON; ADAMS, 1994;

SALVERSON et al., 2002). Até o momento não foram encontrados registros se há diferença em locais de ações ou vias entre os análogos da PGF2α, apesar dos estudos testando suas eficiências. Em síntese, podemos observar que mesmo com todo o progresso obtido nos últimos anos em se compreender o processo de regressão do CL, ainda são necessários mais estudos com o objetivo de esclarecer as vias ativadas durante esse complexo processo.

2.5. miRNAs e funções regulatórias

Com os avanços da biologia molecular, cada dia mais estudos estão sendo realizados para ajudar a elucidar processos por meio de alterações moleculares. Um estudo conduzido por Mondal e colaboradores (2011), usando a técnica de análise de micro-arranjos, mostraram que o uso de PGF2α em diferentes fases (metaestro e diestro) do CL bovino influencia diferentes genes e fatores de transcrição, com maior expressão de genes relacionados ao recrutamento de células imunes e respostas inflamatórias quando a PGF2α foi administrada no diestro. Outro fato encontrado foi que há maior ativação de genes quando a PGF2α foi administrada no metaestro.

No início deste século foram descobertas moléculas com funções regulatórias pós-transcricionais, os microRNAs (miRNAs). Os miRNAs são pequenas moléculas de RNA que possuem em média 22 nucleotídeos e são responsáveis pelo silenciamento da expressão de mRNAs, regulando a produção de proteínas (BARTEL, 2004; KROL et al., 2010). Ao analisar miRNAs em CL de vacas durante todo o ciclo estral, Hossain e colaboradores (2009) conseguiram identificar miRNAs, utilizando método de sequenciamento e posterior detecção utilizando RT-PCR, que estão mais ou menos expressos e alguns dos genes sobre os quais atuam. Contudo, não obtiveram muitas respostas do papel dessas moléculas no metaestro e diestro. Por outro lado, Maalouf et al.(2016) trabalhou com amostras de ovário de vacas no metaestro e diestro, observaram diferenças no perfil de miRNA encontrados, obtendo miRNAs específicos para cada fase, obtendo, por meio de cultura de células *in vitro,* alterações na produção de P4 e ações mitogênicas das células luteais.

Uma recente pesquisa realizada com novilhas taurinas superovuladas com CL obtidos nos dias 7 e 15 do ciclo, compararam a relação entre tamanho/volume do CL, com a quantidade de P4 e a relação da presença de miRNA influenciando em duas

enzimas percursoras da progesterona (CYP11A1 e STAR). Demonstrando que um *cluster* dos miR-183-96-182 é responsável pela regulação esteroidoigênica do CL. A relação entre volume/tamanho com a produção de P4 foi a esperada, contudo, foram encontrados miRNA diferencialmente expressos de acordo com a quantidade de enzimas, evidenciando que, com o tempo, os miRNA do CL vão mudando a expressão e/ou presença (DONADEU et al., 2020). Há também comprovações sobre o efeito de miRNAs no gene responsável pela produção de receptores de ocitocina nas células luteínicas (OXTR). Pesquisadores coletaram amostras de CL em quatro fases: inicial (D1-D4), meio do ciclo (D5-D10), em regressão (D11-D16) e em degeneração (D17-D21) de vacas da raça Simental. Os resultados obtidos foram que a presença do miR-29b é diferentemente expresso durante as fases, promovendo redução na expressão do OXTR, modulando assim a produção de P4 e função do CL (XU et al., 2018). Outro estudo realizado com o objetivo de identificar funções do miRNA na regressão ou não dos CL, possibilitou indicar o miR-378 associado com o processo de apoptose (MA et al., 2011).

3. REFERÊNCIAS BIBLIOGRÁFICAS

ACOSTA, T. J.; YOSHIZAWA, N.; OHTANI, M.; MIYAMOTO, A. Local changes in blood flow within the early and midcycle corpus luteum after prostaglandin F2α injection in the cow. **Biology of Reproduction**, [s. l.], v. 66, n. 3, p. 651–658, 2002. a. Disponível em: <https://pubmed.ncbi.nlm.nih.gov/11870071/>. Acesso em: 1 mar. 2021.

ACOSTA, T. J.; YOSHIZAWA, N.; OHTANI, M.; MIYAMOTO, A. Local changes in blood flow within the early and midcycle corpus luteum after prostaglandin F2α injection in the cow. **Biology of Reproduction**, [s. l.], v. 66, n. 3, p. 651–658, 2002. b.

ALILA, H. W.; HANSEL, W. Origin of Different Cell Types in the Bovine Corpus Luteum as Characterized by Specific Monoclonal Antibodies 1. **Biology of Reproduction**, [s. l.], v. 31, n. 5, p. 1015–1025, 1984. Disponível em: <https://academic.oup .com/biolreprod/article-lookup/doi/10.1095/biolreprod31.5.1015>. Acesso em: 20 jul. 2020.

BARTEL, D. P. **MicroRNAs: Genomics, Biogenesis, Mechanism, and Function**, Cell Press, 2004.

BERISHA, B.; SCHAMS, D.; MIYAMOTO, A. The expression of angiotensin and endothelin system members in bovine corpus luteum during estrous cycle and pregnancy. **Endocrine**, [s. l.], v. 19, n. 3, p. 305–312, 2002.

BERTOLO, P. H. L. Relação entre as lesões histológicas e a carga parasitária da região ungueal de cães naturalmente infectados com Leishmania infantum. [s. l.], 2017.

BOURNE, G. R.; MOSS, S. R.; PHILLIPS, P. J.; SHUKER, B. The metabolic fate of the synthetic prostaglandin cloprostenol (‘Estrumate’) in the cow: Use of ion cluster techniques to facilitate metabolite identification. **Biological Mass Spectrometry**, [s. l.], v. 7, n. 5, p. 226–230, 1980.

BOWOLAKSONO, A.; NISHIMURA, R.; HOJO, T.; SAKUMOTO, R.; ACOSTA, T. J.; OKUDA, K. Anti-apoptotic roles of prostaglandin E2 and F2alpha in bovine luteal steroidogenic cells. **Biology of Reproduction**, [s. l.], v. 79, n. 2, p. 310–317, 2008. Disponível em: <https://pubmed.ncbi.nlm.nih.gov/18463360/>. Acesso em: 21 maio. 2021.

CACHAPUZ, J. M. S. Experiencias com o desmame aos 60 e 90 dias. **Emater**, [s. l.], p. 1–52, 1997.

CARAMBULA, S. F.; MATIKAINEN, T.; LYNCH, M. P.; FLAVELL, R. A.; DIAS GONÇALVES, P. B.; TILLY, J. L.; RUEDA, B. O. R. Caspase-3 is a pivotal mediator of apoptosis during regression of the ovarian corpus luteum. **Endocrinology**, [s. l.], v. 143, n. 4, p. 1495–1501, 2002.

CAROU, M. C.; CRUZANS, P. R.; MARURI, A.; STOCKERT, J. C.; LOMBARDO, D. M. Apoptosis in ovarian granulosa cells of cattle: Morphological features and clearance by homologous phagocytosis. **Acta Histochemica**, [s. l.], v. 117, n. 1, p. 92–103, 2015.

CHACUR, M. G. M.; AURÉLIO, P. T. F.; SCALON JÚNIOR, O.; INAGUE, L.; SCALON, L. F.; KRONKA, S. D. N. Efeitos de baixas doses de cloprostenol via intramuscular ou submucosavulvar na indução do estro e taxas de prenhez em vacas Nelore. **Semina: Ciências Agrárias**, [s. l.], v. 31, n. 2, p. 451, 2010.

CHEN, D. B.; WESTFALL, S. D.; FONG, H. W.; ROBERSON, M. S.; DAVIS, J. S. Prostaglandin F(2α) stimulates the Raf/MEK1/mitogen-activated protein kinase signaling cascade in bovine luteal cells. **Endocrinology**, [s. l.], v. 139, n. 9, p. 3876–3885, 1998. Disponível em: <https://pubmed.ncbi.nlm.nih.gov/9724043/>. Acesso em: 2 mar. 2021.

CHOUDHARY, E.; SEN, A.; INSKEEP, E. K.; FLORES, J. A. Developmental sensitivity of the bovine corpus luteum to prostaglandin F2α (PGF2α) and endothelin-1 (ET-1): Is ET-1 a mediator of the luteolytic actions of PGF2α or a tonic inhibitor of progesterone secretion? **Biology of Reproduction**, [s. l.], v. 72, n. 3, p. 633–642, 2005.

COLAZO, M. G.; MARTINEZ, M.; KASTELIC, J. P.; MAPLETOFT, R. J.; COLAZO, M. G.; FABIAN MARTÍNEZ, M.; PATRICK KASTELIC, J.; MAPLETOFT, R. J. Effects of dose and route of administration of cloprostenol on luteolysis, estrus and ovulation in beef heifers. **Elsevier**, [s. l.], v. 72, p. 47–62, 2002. Disponível em: <https://www.sciencedirect.com/science/article/pii/S0378432002000878>. Acesso em: 31 jan. 2022.

CREIGHTON, C. J. et al. Comprehensivemolecular characterization of clear cell renal cell carcinoma. **Nature**, [s. l.], v. 499, n. 7456, p. 43–49, 2013.

DAMBER, J.-E.; CAJANDER, S.; GÅFVELS, M.; SELSTAM, G. Blood Flow Changes and Vascular Appearance in Preovulatory Follicles and Corpora Lutea in Immature, Pregnant Mare's Serum Gonadotropin-Treated Rats1. **Biology of Reproduction**, [s. l.], v. 37, n. 3, p. 651–658, 1987. Disponível em: <https://academic.oup.com/biolreprod/article-lookup/doi/10.1095/biolreprod37.3.651>. Acesso em: 20 jul. 2020.

DAVIS, J. S.; RUEDA, B. R. The corpus luteum: an ovarian structure with maternal instincts and suicidal tendencies. **Frontiers in bioscience : a journal and virtual library**, [s. l.], v. 7, n. October, 2002.

DE ÁVILA, A.; BRIDI, A.; ANDRADE, G.; DEL COLLADO, M.; SANGALLI, J.; NOCITI, R.; DA SILVA JUNIOR, W.; BASTIEN, A.; ROBERT, C.; MEIRELLES, F.; PERECIN, F.; DA SILVEIRA, J. Estrous cycle impacts miRNA content in extracellular vesicles that modulate bovine cumulus cell transcripts during in vitro maturation Running title: Effect of different estrous cycle on small EVs. **Biology of Reproduction**, [s. l.], 2019.

DE FERRONATO GA, CEREZETTI MB, BRIDI A, PRADO CM, DOS SANTOS G,

BASTOS NM, DA ROSA PMS, FERST JG, Da S. J. MicroRNA Profiling Using a PCR-Based Method. In: **Methods Mol Biol.** [s.l: s.n.]. p. 2595:159–170.

DONADEU, F. X.; SANCHEZ, J. M.; MOHAMMED, B. T.; IOANNIDIS, J.; STENHOUSE, C.; MAIOLI, M. A.; ESTEVES, C. L.; LONERGAN, P. Relationships between size, steroidogenesis and miRNA expression of the bovine corpus luteum. **Theriogenology**, [s. l.], v. 145, n. xxxx, p. 226–230, 2020. Disponível em: <https://doi.org/10.1016/j.theriogenology.2019.10.033>

DONALDSON, L. E. A comparison of cloprostenol and dinoprost tromethamine for the control of estrus in bovine embryo transfer. **Theriogenology**, [s. l.], v. 21, n. 6, p. 1019–1022, 1984.

EL-SHERRY, T. M.; SENOSY, W.; MAHMOUD, G. B.; WASFY, S. I. Effect of dinoprost and cloprostenol on serum nitric oxide and corpus luteum blood flow during luteolysis in ewes. **Theriogenology**, [s. l.], v. 80, n. 5, p. 513–518, 2013.

ETHERINGTON, W. G.; KELTON, D. F.; ADAMS, J. E. Reproductive performance of dairy cows following treatment with fenprostalene, dinoprost, or cloprostenol between 24 and 31 Days post partum: A field trial. **Theriogenology**, [s. l.], v. 42, n. 5, p. 739–752, 1994.

FERRAZ JUNIOR, M. V. C.; PIRES, A. V.; BIEHL, M. V.; SANTOS, M. H.; POLIZEL, D. M.; NEPOMUCENO, D. D.; SARTORI, R.; BARRETO FILHO, J. B.; GONÇALVES, J. R. S.; DAY, M. L. Luteolysis in Bos indicus cows on Days 5 and 7 of estrous cycle with varying doses of PGF2α. **Theriogenology**, [s. l.], v. 86, n. 5, p. 1268–1274, 2016.

FILIPPATOS, G. S.; GANGOPADHYAY, N.; LALUDE, O.; PARAMESWARAN, N.; SAID, S. I.; SPIELMAN, W.; UHAL, B. D. Regulation of apoptosis by vasoactive peptides. **American Journal of Physiology - Lung Cellular and Molecular Physiology**, [s. l.], v. 281, n. 4 25-4, 2001.

FITZ, T. A.; MAYAN, M. H.; SAWYER, H. R.; NISWENDER, G. D. Characterization of Two Steroidogenic Cell Types in the Ovine Corpus Luteum1, 2. **Biology of Reproduction**, [s. l.], v. 27, n. 3, p. 703–711, 1982. Disponível em: <https://pubmed.ncbi.nlm.nih.gov/6291651/>. Acesso em: 20 jul. 2020.

GECAJ, R. M.; SCHANZENBACH, C. I.; KIRCHNER, B.; PFAFFL, M. W.; RIEDMAIER, I.; TWEEDIE-CULLEN, R. Y.; BERISHA, B. The dynamics of microRNA transcriptome in bovine corpus luteum during its formation, function, and regression. **Frontiers in Genetics**, [s. l.], v. 8, n. DEC, p. 213, 2017. Disponível em: <www.frontiersin.org>. Acesso em: 25 ago. 2020.

GINTHER, O. J.; ARAUJO, R. R.; PALHÃO, M. P.; RODRIGUES, B. L.; BEG, M. A. Necessity of Sequential Pulses of Prostaglandin F2alpha for Complete Physiologic Luteolysis in Cattle1. **Biology of Reproduction**, [s. l.], v. 80, n. 4, p. 641–648, 2009. Disponível em: <https://pubmed.ncbi.nlm.nih.gov/19073999/>. Acesso em: 28 jul. 2020.

GINTHER, O. J.; FUENZALIDA, M. J.; SHRESTHA, H. K.; BEG, M. A. Concomitance of luteinizing hormone and progesterone oscillations during the transition from preluteolysis to luteolysis in cattle. **DAE**, [s. l.], v. 40, n. 2, p. 77–86, 2011. Disponível em: <http://dx.doi.org/10.1016/j.domaniend.2010.09.002>

GINTHER, O. J.; SHRESTHA, H. K.; FUENZALIDA, M. J.; SHAHIDUZZAMAN, A. K. M. Intrapulse temporality between pulses of a metabolite of prostaglandin F 2 ⎵ and circulating concentrations of progesterone before , during , and after spontaneous luteolysis in heifers. **THE**, [s. l.], v. 74, n. 7, p. 1179–1186, 2010. Disponível em: <http://dx.doi.org/10.1016/j.theriogenology.2010.05.018>

GINTHER, O. J.; SILVA, L. A.; ARAUJO, R. R.; BEG, M. A. Temporal associations among pulses of 13,14-dihydro-15-keto-PGF 2alpha, luteal blood flow, and luteolysis in cattle. **Biology of Reproduction**, [s. l.], v. 76, n. 3, p. 506–513, 2007. Disponível em: <https://pubmed.ncbi.nlm.nih.gov/17151348/>. Acesso em: 30 jul. 2020.

GIOSO, M. M.; COSTA, E. P. Da; FERNANDES, C. A. de C.; TORRES, C. A. A.; CARVALHO, G. R. De. Perfil de progesterona e intervalo ao estro de receptoras bovinas sincronizadas com doses reduzidas de cloprostenol. **Revista Brasileira de Zootecnia**, [s. l.], v. 34, n. 4, p. 1181–1187, 2005.

GIRSH, E.; MILVAE, R. A.; WANG, W.; MEIDAN, R. Effect of Endothelin-1 on Bovine Luteal Cell Function: Role in Prostaglandin F2α-Induced Antisteroidogenic Action. **Endocrinology**, [s. l.], v. 137, n. 4, p. 1306–1312, 1996. Disponível em: <https://pubmed.ncbi.nlm.nih.gov/8625904/>. Acesso em: 30 jul. 2020.

GRANADOS-VILLARREAL, L. M.; ZARCO, L.; MEJÍA, O.; SÁNCHEZ-TORRES, M. T.; PABLOS-HACH, J. L. Luteolytic efficiency of reduced doses of cloprostenol in the ewe. Effect of progesterone concentrations at the time of treatment. **Animal Reproduction Science**, [s. l.], v. 186, p. 68–76, 2017.

GRIVICICH, I.; REGNER, A.; DA ROCHA, A. B. Morte Celular por Apoptose. **Revista Brasileira de Cancrologia**, [s. l.], v. 53, n. 3, p. 335–343, 2007. Disponível em: <http://www1.inca.gov.br/rbc/n_53/v03/pdf/revisao4.pdf>

HAFEZ, B.; HAFEZ, E. S. E. **Reprodução Animal. 7. ed.** 7. ed. ed. São Paulo: Manole, 2004.

HAYASHI, K.; MIYAMOTO, A. Angiotensin II interacts with prostaglandin F(2α) and endothelin-1 as a local luteolytic factor in the bovine corpus luteum in vitro. **Biology of Reproduction**, [s. l.], v. 60, n. 5, p. 1104–1109, 1999. Disponível em: <https://pubmed.ncbi.nlm.nih.gov/10208970/>. Acesso em: 30 jul. 2020.

HERR, D.; BEKES, I.; WULFF, C. Regulation of endothelial permeability in the corpus luteum: A review of the literature. **Geburtshilfe und Frauenheilkunde**, [s. l.], v. 73, n. 11, p. 1107–1111, 2013.

HOJO, T.; SIEMIENIUCH, M. J.; LUKASIK, K.; PIOTROWSKA-TOMALA, K. K.;

JONCZYK, A. W.; OKUDA, K.; SKARZYNSKI, D. J. Programmed necrosis - a new mechanism of steroidogenic luteal cell death and elimination during luteolysis in cows. **Scientific Reports**, [s. l.], v. 6, p. 1–14, 2016.

HOSSAIN, M.; GHANEM, N.; HOELKER, M.; RINGS, F.; PHATSARA, C.; THOLEN, E.; SCHELLANDER, K.; TESFAYE, D. Identification and characterization of miRNAs expressed in the bovine ovary. **BMC Genomics**, [s. l.], v. 10, n. 1, p. 443, 2009. Disponível em: <https://link.springer.com/articles/10.1186/1471-2164-10-443>. Acesso em: 20 jul. 2020.

HOSSAIN, M. M.; SOHEL, M. M. H.; SCHELLANDER, K.; TESFAYE, D. **Characterization and importance of microRNAs in mammalian gonadal functions**, Springer, 2012. Disponível em: <https://link.springer.com/article/10.1007/s00441-012-1469-6>. Acesso em: 20 jul. 2020.

JG, C. **Tratado de fisiologia veterinária**. Rio de Janeiro: Guanabara Koogan, [s.d.].

KAYA, S.; KAÇAR, C.; POLAT, B.; ÇOLAK, A.; KAYA, D.; GÜRCAN, S.; BOLLWEIN, H.; ASLAN, S. Association of luteal blood flow with follicular size, serum estrogen and progesterone concentrations, and the inducibility of luteolysis by PGF2α in dairy cows. **Theriogenology**, [s. l.], v. 87, p. 167–172, 2017.

KINDHAL, H.; LINDELL, J. O.; EDQVIST, L. E. Release of prostaglandin F2α during oestrus cycle. **Acta Veterinaria Scandinavica**, [s. l.], v. 77, p. 143–58, 1981.

KNICKERBOCKER, J. J.; WILTBANK, M. C.; NISWENDER, G. D. Mechanisms of luteolysis in domestic livestock. **Domestic Animal Endocrinology**, [s. l.], v. 5, n. 2, p. 91–107, 1988.

KOBAYASHI, S.; BERISHA, B.; AMSELGRUBER, W. M.; SCHAMS, D.; MIYAMOTO, A. Production and localisation of angiotensin II in the bovine early corpus luteum: a possible interaction with luteal angiogenic factors and prostaglandin F2 alpha. **The Journal of endocrinology**, [s. l.], v. 170, n. 2, p. 369–380, 2001. Disponível em: <https://pubmed.ncbi.nlm.nih.gov/11479133/>. Acesso em: 4 dez. 2022.

KORZEKWA, A. J.; LUKASIK, K.; PILAWSKI, W.; PIOTROWSKA-TOMALA, K. K.; JAROSZEWSKI, J. J.; YOSHIOKA, S.; OKUDA, K.; SKARZYNSKI, D. J. Influence of prostaglandin F2α analogues on the secretory function of bovine luteal cells and ovarian arterial contractility in vitro. **Veterinary Journal**, [s. l.], v. 199, n. 1, p. 131–137, 2014. Disponível em: <http://dx.doi.org/10.1016/j.tvjl.2013.09.021>

KORZEKWA, A. J.; OKUDA, K.; WOCLAWEK-POTOCKA, I.; MURAKAMI, S.; SKARZYNSKI, D. J. Nitric oxide induces apoptosis in bovine luteal cells. **Journal of Reproduction and Development**, [s. l.], v. 52, n. 3, p. 353–361, 2006. Disponível em: <https://pubmed.ncbi.nlm.nih.gov/16493180/>. Acesso em: 21 maio. 2021.

KROL, J.; BUSSKAMP, V.; MARKIEWICZ, I.; STADLER, M. B.; RIBI, S.; RICHTER, J.; DUEBEL, J.; BICKER, S.; FEHLING, H. J.; SCHÜBELER, D.; OERTNER, T. G.;

SCHRATT, G.; BIBEL, M.; ROSKA, B.; FILIPOWICZ, W. Characterizing Light-Regulated Retinal MicroRNAs Reveals Rapid Turnover as a Common Property of Neuronal MicroRNAs. **Cell**, [s. l.], v. 141, n. 4, p. 618–631, 2010.

MA, T.; JIANG, H.; GAO, Y.; ZHAO, Y.; DAI, L.; XIONG, Q.; XU, Y.; ZHAO, Z.; ZHANG, J. Microarray analysis of differentially expressed microRNAs in non-regressed and regressed bovine corpus luteum tissue; microRNA-378 may suppress luteal cell apoptosis by targeting the interferon gamma receptor 1 gene. **Journal of Applied Genetics**, [s. l.], v. 52, n. 4, p. 481–486, 2011. Disponível em: <https://link.springer.com/article/10.1007/s13353-011-0055-z>. Acesso em: 27 jul. 2020.

MAALOUF, S. W.; SMITH, C. L.; PATE, J. L. Changes in microRNA expression during maturation of the bovine corpus luteum: Regulation of luteal cell proliferation and function by microRNA-34a. **Biology of Reproduction**, [s. l.], v. 94, n. 3, 2016. Disponível em: <https://pubmed.ncbi.nlm.nih.gov/26864197/>. Acesso em: 17 ago. 2020.

MARTIN, I.; FERREIRA, J. C. P. Fisiologia da ovulação e da formação do corpo lúteo bovino. **Veterinária e Zootecnia**, [s. l.], v. 16, n. 2, p. 270–279, 2009.

MARTIN, S. J. Caspases: Executioners of Apoptosis. **Pathobiology of Human Disease: A Dynamic Encyclopedia of Disease Mechanisms**, [s. l.], v. 16, p. 145–152, 2014.

MARTINS, J.; POLICELLI, R.; NEUDER, L.; … W. R.-J. of dairy; 2011, Undefined. Effects of cloprostenol sodium at final prostaglandin F2α of Ovsynch on complete luteolysis and pregnancy per artificial insemination in lactating dairy cows. **Elsevier**, [s. l.], [s.d.]. Disponível em: <https://www.sciencedirect.com/science/article/pii/S0022030211002694>. Acesso em: 31 jan. 2022.

MCBRIDE, D.; CARRÉ, W.; SONTAKKE, S. D.; HOGG, C. O.; LAW, A.; DONADEU, F. X.; CLINTON, M. Identification of miRNAs associated with the follicular-luteal transition in the ruminant ovary. **Reproduction**, [s. l.], v. 144, n. 2, p. 221–233, 2012. Disponível em: <http://ovary.stanford.edu/>. Acesso em: 29 ago. 2020.

MCCRACKEN, J. A.; CUSTER, E. E.; LAMSA, J. C. Luteolysis: A neuroendocrine-mediated event. **Physiological Reviews**, [s. l.], v. 79, n. 2, p. 263–323, 1999. Disponível em: <https://pubmed.ncbi.nlm.nih.gov/10221982/>. Acesso em: 28 jul. 2020.

MEIRA, C.; PESSOA, V. M.; FERREIRA, J. C. P.; ARAUJO, G. H. M.; GIOSO, M. M.; BICUDO, S. D.; OBA, E.; ORLANDI, C. Alternative low doses and routes of administering a prostaglandin F2α analogue to induce luteolysis in Nelore cows. **Journal of Veterinary Science**, [s. l.], v. 7, n. 4, p. 387–390, 2006.

MILVAE, R. A. Inter-relationships between endothelin and prostaglandin F2α in corpus luteum function. **Reviews of Reproduction**, [s. l.], v. 5, n. 1, p. 1–5, 2000. Disponível

em: <https://pubmed.ncbi.nlm.nih.gov/10711729/>. Acesso em: 20 jul. 2020.

MIYAMOTO, A.; SHIRASUNA, K.; SASAHARA, K. **Local regulation of corpus luteum development and regression in the cow: Impact of angiogenic and vasoactive factors**, 2009.

MONDAL, M.; SCHILLING, B.; FOLGER, J.; STEIBEL, J. P.; BUCHNICK, H.; ZALMAN, Y.; IRELAND, J. J.; MEIDAN, R.; SMITH, G. W. Deciphering the luteal transcriptome: Potential mechanisms mediating stage-specific luteolytic response of the corpus luteum to prostaglandin F2α. **Physiological Genomics**, [s. l.], v. 43, n. 8, p. 447–456, 2011. Disponível em: <https://pubmed.ncbi.nlm.nih.gov/21325060/>. Acesso em: 2 ago. 2020.

NASCIMENTO, A. B.; SOUZA, A. H.; KESKIN, A.; SARTORI, R.; WILTBANK, M. C. Lack of complete regression of the Day 5 corpus luteum after one or two doses of PGF2α in nonlactating Holstein cows. **Theriogenology**, [s. l.], v. 81, n. 3, p. 389–395, 2014. a. Disponível em: <http://dx.doi.org/10.1016/j.theriogenology.2013.10.009>

NASCIMENTO, A. B.; SOUZA, A. H.; KESKIN, A.; SARTORI, R.; WILTBANK, M. C. Lack of complete regression of the Day 5 corpus luteum after one or two doses of PGF2α in nonlactating Holstein cows. **Theriogenology**, [s. l.], v. 81, n. 3, p. 389–395, 2014. b.

NASH, A. D.; BACA, M.; WRIGHT, C.; SCOTNEY, P. D. The biology of vascular endothelial growth factor-B (VEGF-B). **Pulmonary Pharmacology and Therapeutics**, [s. l.], v. 19, n. 1, p. 61–69, 2006.

NISHIMURA, R.; KOMIYAMA, J.; … Y. T.-B. of; 2008, Undefined. Hypoxia promotes luteal cell death in bovine corpus luteum. **academic.oup.com**, [s. l.], [s.d.]. Disponível em: <https://academic.oup.com/biolreprod/article-abstract/78/3/529/2630260>. Acesso em: 31 jan. 2022.

NISWENDER, G. D.; JUENGEL, J. L.; SILVA, P. J.; ROLLYSON, M. K.; MCINTUSH, E. W. **Mechanisms Controlling the Function and Life Span of the Corpus Luteum**. [s.l: s.n.].

NISWENDER, G. D.; JUENGEL, J. L.; SILVA, P. J.; ROLLYSON, M. K.; MCINTUSH, E. W. Mechanisms controlling the function and life span of the corpus luteum. **Physiological Reviews**, [s. l.], v. 80, n. 1, p. 1–29, 2000. b.

O'SHEA, J. D.; RODGERS, R. J.; D'OCCHIO, M. J. Cellular composition of the cyclic corpus luteum of the cow. **Journal of Reproduction and Fertility**, [s. l.], v. 85, n. 2, p. 483–487, 1989. Disponível em: <https://pubmed.ncbi.nlm.nih.gov/2703988/>. Acesso em: 20 jul. 2020.

PELUFFO, M. C.; BUSSMANN, L.; STOUFFER, R. L.; TESONE, M. Expression of caspase-2, -3, -8 and -9 proteins and enzyme activity in the corpus luteum of the rat at diferent stages during the natural estrous cycle. **Reproduction**, [s. l.], v. 132, n. 3, p.

465–475, 2006.

PUGLIESI, G.; NAVES, J. Regressão Espontânea Do Corpo Lúteo Em Bovinos-Revisão Spontaneous Corpus Luteum Regression in Cattle : Review Revisão Spontaneous Corpus Luteum Regression in Cattle : Review. [s. l.], n. August, p. 1–12, 2017.

PUGLIESI, G.; REZENDE, R. G.; SILVA, J. C. B. Da; LOPES, E.; NISHIMURA, T. K.; BARUSELLI, P. S.; MADUREIRA, E. H.; BINELLI, M. Use of Doppler ultrasonography in timed-AI and ET programs in cattle. / Uso da ultrassonografia Doppler em programas de IATF e TETF em bovinos. **Revista Brasileira de Reprodução Animal**, [s. l.], v. 41, n. 1, p. 140–150, 2017. Disponível em: <http://search.ebscohost.com/login.aspx?direct=true&db=lbh&AN=20173193194&lang=es&site=ehost-live%0Ahttp://www.cbra.org.br/portal/downloads/publicacoes/rbra/v41/n1/p140-150 (RB662).pdf%0Aemail: gpugliesi@usp.br>

PURSLEY, J. R.; MARTINS, J. P. N.; WRIGHT, C.; STEWART, N. D. Compared to dinoprost tromethamine, cloprostenol sodium increased rates of estrus detection, conception and pregnancy in lactating dairy cows on a large commercial dairy. **Theriogenology**, [s. l.], v. 78, n. 4, p. 823–829, 2012.

PURSLEY, J. R.; MEE, M. O.; WILTBANK, M. C. Synchronization of ovulation in dairy cows using PGF2α and GnRH. **Theriogenology**, [s. l.], v. 44, n. 7, p. 915–923, 1995.

REEVES, P. R. Distribution, Elimination, and Residue Studies in the Cow with the Synthetic Prostaglandin Estrumate. **Journal of Agricultural and Food Chemistry**, [s. l.], v. 26, n. 1, p. 152–155, 1978.

SALVERSON, R. R.; DEJARNETTE, J. M.; MARSHALL, C. E.; WALLACE, R. A. Synchronization of estrus in virgin beef heifers using melengestrol acetate and PGF2α: an efficacy comparison of cloprostenol and dinoprost tromethamine. **Theriogenology**, [s. l.], v. 57, n. 2, p. 853–858, 2002.

SARTORI, R.; HAUGHIAN, J. M.; SHAVER, R. D.; ROSA, G. J. M.; WILTBANK, M. C. Comparison of ovarian function and circulating steroids in estrous cycles of Holstein heifers and lactating cows. **Journal of Dairy Science**, [s. l.], v. 87, n. 4, p. 905–920, 2004. Disponível em: <http://dx.doi.org/10.3168/jds.S0022-0302(04)73235-X>

SCHAMS, D.; BERISHA, B.; NEUVIANS, T.; AMSELGRUBER, W.; KRAETZL, W. D. Real-time changes of the local vasoactive peptide systems (angiotensin, endothelin) in the bovine corpus luteum after induced luteal regression. **Molecular Reproduction and Development**, [s. l.], v. 65, n. 1, p. 57–66, 2003. Disponível em: <https://pubmed.ncbi.nlm.nih.gov/12658634/>. Acesso em: 4 mar. 2021.

SENGER, P. L. **Pathways to Pregnancy and Partyritions**. 2nd. ed. [s.l.] : Washington : Current Conceptions Inc, 2003.

SHIRASUNA, K.; AKABANE, Y.; BEINDORFF, N.; NAGAI, K.; SASAKI, M.; SHIMIZU,

T.; BOLLWEIN, H.; MEIDAN, R.; MIYAMOTO, A. Expression of prostaglandin F 2α (PGF 2α) receptor and its isoforms in the bovine corpus luteum during the estrous cycle and PGF 2α-induced luteolysis. **Domestic Animal Endocrinology**, [s. l.], v. 43, n. 3, p. 227–238, 2012. Disponível em: <http://dx.doi.org/10.1016/j.domaniend.2012.03.003>

SHIRASUNA, K.; SASAHARA, K.; MATSUI, M.; SHIMIZU, T.; MIYAMOTO, A. Prostaglandin F2α differentially affects mRNA expression relating to angiogenesis, vasoactivation and prostaglandins in the early and mid corpus luteum in the cow. **Journal of Reproduction and Development**, [s. l.], v. 56, n. 4, p. 428–436, 2010.

SIQUEIRA, L. G. B.; TORRES, C. A. A.; AMORIM, L. S.; SOUZA, E. D.; CAMARGO, L. S. A.; FERNANDES, C. A. C.; VIANA, J. H. M. Interrelationships among morphology, echotexture, and function of the bovine corpus luteum during the estrous cycle. **Animal Reproduction Science**, [s. l.], v. 115, n. 1–4, p. 18–28, 2009.

STELLFLUG, J. N.; LOUIS, T. M.; GOREWIT, R. C.; OXENDER, W. D.; HAFS, H. D. Luteolysis induced by prostaglandin F 2(α) before and after hysterectomy in heifers. **Biology of Reproduction**, [s. l.], v. 17, n. 4, p. 535–540, 1977.

STEVENS, R. D.; SEGUIN, B. E.; MOMONT, H. W. Evaluation of the effects of route of administration of cloprostenol on synchronization of estrus in diestrous dairy cattle. **Journal of the American Veterinary Medical Association**, [s. l.], v. 207, n. 2, p. 214–216, 1995. Disponível em: <https://europepmc.org/article/med/7601719>. Acesso em: 4 dez. 2022.

STEVENSON, J. S.; PHATAK, A. P. Rates of luteolysis and pregnancy in dairy cows after treatment with cloprostenol or dinoprost. **Theriogenology**, [s. l.], v. 73, n. 8, p. 1127–1138, 2010.

STOCCO, C.; TELLERIA, C.; GIBORI, G. The molecular control of corpus luteum formation, function, and regression. **Endocrine Reviews**, [s. l.], v. 28, n. 1, p. 117–149, 2007.

TAI, C. J.; KANG, S. K.; CHOI, K. C.; TZENG, C. R.; LEUNG, P. C. K. Role of mitogen-activated protein kinase in prostaglandin F2α action in human granulosa-luteal cells. **Journal of Clinical Endocrinology and Metabolism**, [s. l.], v. 86, n. 1, p. 375–380, 2001.

TIZARD, I. R. **Imunologia Veterinária**. 9a ed. ed. Rio de Janeiro: Elsevier, 2014.

TREVISOL, E.; FERREIRA, J. C.; ACKERMANN, C. L.; DESTRO, F. C.; MARQUES FILHO, W. C.; CARMAGOS, A. S.; BIEHL, M. V.; DO AMARAL, J. B.; DE FIGUEIREDO PANTOJA, J. C.; SARTORI, R.; FERREIRA, J. C. P. Luteal changes after treatment with sub-luteolytic doses of prostaglandin (cloprostenol sodium) in cattle. **Animal Reproduction Science**, [s. l.], v. 153, p. 8–12, 2015.

TREVISOL, E.; FERREIRA, J. C. P.; ACKERMANN, C. L.; DESTRO, F. C.; AMARAL,

J. B. **Luteólise em bovinos: revisão Luteolysis in cattle: reviewRev. Bras. Reprod. Anim**. [s.l: s.n.]. Disponível em: <www.cbra.org.br>. Acesso em: 20 jul. 2020.

TREVISOL, E.; MOGOLLÓN GARCÍA, H. D.; ACKERMANN, C. L.; LACERDA, W.; PIRES, R. M. L.; LAUFER-AMORIN, R.; CARVALHO, R. F.; FRANCHI, F. F.; CASTILHO, A. C. S.; RIZZOTO, G.; KASTELIC, J. P.; FERREIRA, J. C. P. Partial luteolysis during early diestrus in cattle downregulates VEGFA expression and reduces large luteal cell and corpus luteum sizes and plasma progesterone concentration. **Theriogenology**, [s. l.], v. 158, p. 188–195, 2020.

TSAI, S.-J.; WILTBANK, M. C. Prostaglandin F2α Regulates Distinct Physiological Changes in Early and Mid-Cycle Bovine Corpora Lutea1. **Biology of Reproduction**, [s. l.], v. 58, n. 2, p. 346–352, 1998. Disponível em: <https://academic.oup .com/biolreprod/article-lookup/doi/10.1095/biolreprod58.2.346>. Acesso em: 20 jul. 2020.

UMAÑA SEDÓ, S. G.; FIGUEIREDO, C. C.; GONZALEZ, T. D.; DUARTE, G. A.; UGARTE MARIN, M. B.; CRAWFORD, C. A.; POHLER, K. G.; CHEBEL, R. C.; BILBY, T. R.; BISINOTTO, R. S. Evaluation of luteolysis, follicle size, and time to ovulation in Holstein heifers treated with two different analogs and doses of prostaglandin-F2α. **Journal of Dairy Science**, [s. l.], v. 105, n. 6, p. 5506–5518, 2022.

WAITE, A. L.; HOLTAN, D. W.; STORMSHAK, F. Changes in bovine luteal progesterone metabolism in response to exogenous prostaglandin F2α. **Domestic Animal Endocrinology**, [s. l.], v. 28, n. 2, p. 162–171, 2005.

WILTBANK, M. C. Cell types and hormonal mechanisms associated with mid-cycle corpus luteum function. **Journal of animal science**, [s. l.], v. 72, n. 7, p. 1873–1883, 1994.

WJ., M. Treatment of sheep with prostaglandin F2 alpha enhances production of a luteal chemoattractant for eosinophils. **Am J Reprod Immunol Microbiol.**, [s. l.], v. 15(2), p. :52-6, 1987.

WU, J.; LIU, J.; DING, Y.; ZHU, M.; LU, K.; ZHOU, J.; XIE, X.; XU, Y.; SHEN, X.; CHEN, Y.; SHAO, X.; ZHU, C. MiR-455-3p suppresses renal fibrosis through repression of ROCK2 expression in diabetic nephropathy. **Biochemical and Biophysical Research Communications**, [s. l.], v. 503, n. 2, p. 977–983, 2018.

XU, M. Q.; JIANG, H.; ZHANG, L. Q.; SUN, X. L.; LUO, D.; FU, Y.; GAO, Y.; YUAN, B.; ZHANG, J. B. MiR-29b affects the secretion of PROG and promotes the proliferation of bovine corpus luteum cells. **PLoS ONE**, [s. l.], v. 13, n. 4, 2018. Disponível em: <https://pubmed.ncbi.nlm.nih.gov/29617446/>. Acesso em: 17 ago. 2020.

YADAV, V. K.; LAKSHMI, G.; MEDHAMURTHY, R. Prostaglandin F2α-mediated activation of apoptotic signaling cascades in the corpus luteum during apoptosis: Involvement of caspase-activated DNase. **Journal of Biological Chemistry**, [s. l.], v.

280, n. 11, p. 10357–10367, 2005. Disponível em: <http://dx.doi.org/10.1074/jbc.M409596200>

ZHAN, T.; HUANG, X.; TIAN, X.; CHEN, X.; DING, Y.; LUO, H.; ZHANG, Y. Downregulation of MicroRNA-455-3p Links to Proliferation and Drug Resistance of Pancreatic Cancer Cells via Targeting TAZ. **Molecular Therapy - Nucleic Acids**, [s. l.], v. 10, n. March, p. 215–226, 2018. Disponível em: <https://doi.org/10.1016/j.omtn.2017.12.002>

ZHENG, J.; LIN, Z.; ZHANG, L.; CHEN, H. MicroRNA-455-3p inhibits tumor cell proliferation and induces apoptosis in HCT116 human colon cancer cells. **Medical Science Monitor**, [s. l.], v. 22, p. 4431–4437, 2016.

CAPÍTULO 2 – Artigo elaborado para ser submetido à revista Theriogenology

MORPHOPHYSIOLOGICAL AND MOLECULAR CHANGES IN BOVINE CORPUS LUTEUM AFTER ADMINISTRATION OF DIFFERENT PROSTAGLANDINS AND DOSES IN METAESTRUS AND DIESTRUS

Marina Anchieta Trevisoli[a#], Gabriel Artur Marciano do Nascimento[ab#], Ana Clara Degan Mattos[a], Rosemeri de Oliveira Vasconcelos[a], Paulo Henrique Leal Bertolo[a], Vanessa Garcia Rizzi Mussi[b], Rafael Rodrigues Corrêa[c], Cláudia Cristina Paro de Paz[d], Guilherme de Paula Nogueira[e], Natália Marins Bastos[f], Juliano Coelho da Silveira[f], Lindsay Unno Gimenes[a*]

[a]Department of Pathology, Theriogenology and One Health, FCAV, UNESP, Jaboticabal, Brazil; [b]Ouro Fino Saúde Animal, Cravinhos, Brazil; [c]WTA, Cravinhos, Brazil; [d]Institute of Animal Science, APTA Beef Cattle Center, Sertãozinho, Brazil; [e]Department of Animal Production and Health, FMVA, UNESP, Araçatuba, Brazil; [f]Molecular Morphophysiology and Development Laboratory, FMVZ, USP, Pirassununga, Brazil.

[#]the two first authors contributed equally to this article

*** Corresponding author:** Lindsay Unno Gimenes, Faculdade de Ciências Agrárias e Veterinárias (FCAV), Universidade Estadual Paulista (UNESP), Department of Pathology, Reproduction and Unified Health, Reproduction Biotechnology Laboratory (LABOR), Access Route Professor Paulo Donato Castellane s/n, 14884-900, Jaboticabal, São Paulo, SP, Brazil. E-mail: lindsay.gimenes@unesp.br

ABSTRACT

The objective of the present study was to investigate the processes related to the administration of different prostaglandins (sodium cloprostenol - CS and dinoprost tromethamine - DT) using 100% and 50% of the recommended dose, during metestrus and diestrus (4 and 11 days after ovulation (D0), respectively). The following features were analyzed: luteal dynamics, CL vascularization, quantification of pixels in CL blood perfusion and serum progesterone (P4) measurement (Exp.1) and luteal cell morphometry, numerical value of pixels (NVP) and heterogeneity associated to CL caspase-3 immunostaining, P4 and microRNA (miRNA) expression (Exp.2). In Exp. 1, 44 females had synchronized ovulation and received the following treatments: D4 (CS50% n= 5; CS100% n= 5; DT50% n= 5; DT100% n= 5) and D11 (CS50% n= 7; CS100% n= 5; DT50% n= 6; DT100% n= 6). In Exp. 2, 23 females were synchronized, allocated to treatments: D4 (CS 50%, n=3; CS 100%, n=3; DT 50%, n=3; DT 100%, n=3) and D11 (CS 50%, n=3; CS 100%, n=3; DT 50%, n=3; DT 100%, n=2) and were

slaughtered two days later. Data were analyzed by ANOVA in a factorial arrangement (2x2, in Exp. 1 and Exp. 2) with repeated measurements over time (except for morphometry and immunostaining) and Tukey's test, with significance at < 5%. The miRNA analysis was descriptive. At metestrus, there was an initial reduction in P4, regardless of the drug used and dose used, returning its steroidogenic capacity after 96h (Exp.1). When 100% was used, there was a decline in P4 and a reduction in CL blood perfusion. When 50% of the dose and DT were used, a greater reduction in the area of small luteal cells was observed, while the 50%DT treatment had a greater heterogeneity. CS100% had a greater reduction in P4 (Exp.2), higher NVP, indicating a luteolytic process. In the diestrus phase, both 50% and 100% of the dose of both PGF2α decreased the serum level of P4, vascularization, blood perfusion, and CL size (Exp.1). DT and 100% dose achieved greater reduction of large luteal cells. The DT100% treatment had lower NVP, while CS100% in higher heterogeneity. It was possible to identify 18 unique miRNAs in metestrus, none in diestrus and 5 in common when 50% of the dose was used, regardless of PGFα. With 100% of the dose, none were found in metestrus, 8 miRNAs in diestrus and 17 miRNAs in common. The administration of luteolytics in D4 was suggestive of partial luteolysis when 100% of the dose was used. Administration on D11 was efficient in inducing complete luteolysis, using 50% or 100% of the recommended dose, regardless of the drug.

Key Words: corpus luteum, miRNA, PGF2α, luteolytic pathways

1. INTRODUCTION

The luteolysis process, crucial to promote a new ovulation, occurs due the action of prostaglandin F2α (PGF2α). If pregnancy does not occur around the 17th day after ovulation, the pulsatile release of PGF2α begins in the endometrium, which will promote luteolysis [1]. Luteolysis can be classified as functional and structural, which occurs due to the decline in progesterone levels (P4) and when there is a reduction in the size of the corpus luteum (CL), respectively [2,3]. With the advances of reproductive biotechnology, the use of PGF2α analogues has become important. The most popular analogues are cloprostenol sodium (CS) and dinoprost tromethamine (DT). Several authors have observed similarity between these compounds in estrus induction, conception rate and services per conception [4–6]. However, other researchers have demonstrated differences between them, such as greater efficiency of DT in inducing luteal regression [4] and higher pregnancy rate when using CS in estrous synchronization [7,8]. Due to similar results using different types of PGF2α, studies were initiated to evaluate the luteolytic efficiency when different doses were used. It was observed that twice the dose recommended by the

manufacturer (200%) was equally efficient in CL regression when compared to the use of 50% of the recommended dose in diestrus. However, when less than 25% of the recommended dose was used, only partial luteolysis occurred[9,10].

The phase of the estrous cycle in which the PGF2α analogue is administered has also been studied. Although studies demonstrate the presence of PGF2α receptors on steroidoigenic cells in the CL in the metestrus phase (up to the 5th day after ovulation), there is no regression of the CL when PGF2α is administered [11]. However, when PGF2α is administered in the diestrus phase, complete luteal regression can be observed [9,12,13].

PGF2α is just one of multiple factors that participate in the luteolysis process. Other factors such as oxytocin, estradiol, angiogenic factors (VEFG and FGF) and vasoactive factors (endothelin-1 (ENDT1), nitric oxide (NO) and angiotensin II) are relevant to the luteolytic process, to promote cell apoptosis (reviewed by [14]). Apoptosis is a process characterized by the death and remodeling of the cellular matrix (reviewed by [15]), governed by the intrinsic and extrinsic pathways. When cellular stress occurs, such as hypoxia, the intrinsic pathway is activated, releasing pro-apoptotic molecules through mitochondria. The extrinsic pathway is activated by specific ligands in tumor necrosis receptors (rTNF) and then caspase cascades are activated, which play an important role in CL apoptosis[15,16].

All these processes, both formation, activation of the luteolytic process and regression, are modulated by genes and proteins, but appear to also be regulated by microRNAs (miRNAs) [17,18]. miRNAs are small, non-coding RNA molecules that regulate pathways by modulating protein translation [19]. Studies have demonstrated differences in the expression of various miRNAs between diestrus and metestrus phases [20]. Recently, the relationship between mir-29b and modulation of P4 production [21] and miR-378 with apoptotic processes [22] was found. However, it has not yet been possible to associate which miRNAs are regulating pathways under different conditions of luteolytic induction.

Therefore, the objective of the present study was to evaluate the functional, structural and molecular changes of the CL after the administration of two analogues and two different dosages of PGF2α, in the metestrus and diestrus phases.

2. MATERIAL AND METHODS

All procedures were approved by the Animal Use Ethics Committee of the Universidade Estadual Paulista “Júlio Mesquita Filho” – UNESP Jaboticabal (protocol no. 006001/18).

This article is a compilation of co-authored data, so the methodology is based on master's thesis of Nascimento (2019)[23].

2.1. Experiment 1

2.1.1. Animals

Fourty four bovine females, Nelore and crossbreeds, nulliparous and multiparous, with an average age of 35.0 ± 2.1 months and an average weight of 392.3 ± 8.2 kg were used. Only cyclic non-lactating females were selected (confirmed by two evaluations ultrasound examinations at a 10-days interval, prior to the beginning of the experiment), with a body condition score (BCS) ≥2.75 (on a scale of 1 to 5) [24], from the João Martins farm, Guatapará – SP (21o29'48” S-48º02'16” W).

The animals were kept in *Brachiara brizantha* pasture with free access to water and mineral supplementation.

2.1.2. Experimental Design

The design was completely randomized, with a factorial arrangement of treatments: 2 (PGF2α analogues: dinoprost tromethamine and cloprostenol sodium) x 2 (PGF2α doses: 50% and 100% of the dose recommended by the fabricant) at two different moments of the estrous cycle: metestrus (D4) and diestrus (D11); considering day 0 as the day of ovulation)

The study was carried out in two replicates, with an interval of 77 days. Prior to the beginning of treatments with prostaglandins, ovulation was synchronized with a protocol based on estrogen and progesterone, to obtain two simultaneous groups of animals, referring to metestrus (D4) and diestrus (D11) groups. On D-11, 2mg of estradiol benzoate and an intravaginal progesterone device were administered. The device was removed and estradiol cypionate and sodium cloprostenol were administered seven days later. From 60 hours after

removal of the intravaginal device, ultrasound monitoring was carried out every 12 hours , to include in the study only animals ovulated between 72 and 84 hours. After confirming ovulation, the animals were randomized according to BCS (mean 3.11 ± 0.04), breed and CL diameter (mean 1.62 ± 0.04 cm), to receive the following treatments: D4 (CS50% n= 5; CS100% n= 5; DT50% n= 5; DT100% n= 5) and D11 (CS50% n= 7; CS100% n= 5; DT50% n= 6; DT100% n= 6).

2.1.3. Blood sampling and P4 analysis

Blood samples (10 mL) were collected by puncture of the jugular vein using vacuum tubes without anticoagulant (Vaccutainer®, BD, Franklin Lakes, NJ, USA). Samples were collected before treatment with PGF2 (0 h), 8, 24, 48, 72 and 96 h later, centrifuged at 2086 x g for 15 minutes, aliquoted in duplicate in 2.0 mL microtubes (Eppendorf ®) and immediately stored in a freezer at -20ºC until analysis. P4 measurement was carried out at the Animal Endocrinology Laboratory of the Faculty of Veterinary Medicine of the Universidade Estadual Paulista – Araçatuba Campus. Serum progesterone concentrations were determined using a commercial bovine radioimmunoassay technique kit (ICN Pharmaceuticals, Inc., Costa Mesa, CA, USA). The limit of quantification and detection was 0.290 and 0.068 ng/mL, respectively. The intra- and inter-assay coefficient of variation was 7.17% and 11.74%, respectively.

2.1.4. Ultrasonographic Evaluations and Computerized Analysis of the CL

Ultrasound assessments were performed to detect the time of ovulation, as described in item 2.1.2, using B mode. To evaluate luteal dynamics, B mode and the Color Doppler function were used, starting before treatment with PGF2 (0 h), 24, 48, 72 and 96 h later. All measures were performed by the same operator, using a portable ultrasound device (Z5 VET with 5MHz linear transducer, Mindray Medical International, China).

The CL area was calculated using the B-mode trace function. For evaluations using the Doppler function, the device transducer was configured with a frequency of 5.0 MHz, constant color gain settings (70), wall filter (309) and blood flow detection speed (5 cm/sec). Vascularization scores were estimated at the time of the evaluations, following the classification below, adapted from the criteria described by Pugliese et al. (2017) [25]: CL

vascularization - score 0: absence of colored signs in the CL, score 1: filling up to 25% of the CL with colored signs; score 2: filling 26 to 50% of the CL with colored signs; score 3: filling 51 to 75% of the CL with colored signs; score 4: filling 76 to 100% of the CL with colored signs.

To analyze the variables obtained from the ultrasound evaluations, individual videos of each CL were recorded, lasting 5 seconds, using the cineloop function. The recorded videos captured both with B-mode and Doppler images, comprising sections that exhibited the largest diameter and maximum vascularization of the CL. All images were analyzed using the Image J 1.50e computer program (National Institutes of Health), by which the total number of pixels and the number of pixels in the vascularized area of the CL were obtained. By obtaining these two values, it was possible to calculate the CL vascular perfusion percentage, using the following formula: % vascular perfusion = (n of colored pixels/total number of pixels) x 100.

2.2. EXPERIMENT 2

2.2.1. Animals

Twenty-three Nelore and crossbreed females, with average age of 54.0 ± 3.0 months and average weight of 492.2 ± 17.2 kg were used. Only cyclic non-lactating females were selected (confirmed by two ultrasound evaluations in a 10 days interval, before the beginning of the experiment), with a body condition score (BCS) ≥2.75 (on a scale of 1 to 5) [24].

The animals were maintained with the same nutritional treatment and location as the animals in 2.1.1.

2.2.2. Experimental Desing

The selection and ovulation synchronization criteria for the distribution of treatments were the same as those described in 2.1.2.. The day of ovulation was considered as D0. Four (D4) or eleven (D11) days after ovulation, the animals were randomized according to BCS (mean 3.66 ± 0.02), breed and CL diameter (mean 1.44 ± 0.07 cm) and distributed in the following treatments: D4 (CS 50%, n=3; CS 100%, n=3; DT 50%, n=3; DT 100%, n=3) and D11 (CS 50%, n=3; CS

100%, n=3; DT 50%, n=3; DT 100%, n=2). The females were slaughtered 48 hours after the treatments.

2.2.3. Ultrassonographic Evaluations

Ultrasound evaluations were performed to detect the time of ovulation and to randomize the experimental groups immediately before treatment with PGF2 (0 h; Figure 2), as described in 2.1.3, using B mode.

2.2.4. Blood Sampling and P4 Analysis

The sample collection, processing and storage procedures, as well as the determination of progesterone concentrations, were carried out as described in 2.1.4. Samples were collected before treatment with PGF2α (0 h) and 24 h later. The limit of quantification and detection was 0.290 and 0.068 ng/mL, respectively. The intra- and inter-assay coefficient of variation was 7.17% and 11.74%, respectively.

2.2.5. Ovary collection

After slaughtering the animals, the ovary containing the CL was removed and divided into two parts for further analysis. One part was placed in a universal collection bottle containing 10% paraformaldehyde solution (PAF) pH 7.0, for immunohistochemistry analysis, and the other in microtubes stored in liquid nitrogen, for miRNA expression analysis.

2.2.6. Corpus luteum preparation and immunohistochemistry slides confection

The material was processed at the Histopathology Laboratory of the Department of Pathology, Theriogenology and One Health at the Universidade Estadual Paulista – Jaboticabal Campus. The corpus luteum was isolated, fractionated and the obtained fragments were stored in PAF for up to 72 h and then washed with PBS solution pH 7.5. Subsequently, the tissues were dehydrated in a sequence of alcoholic solutions in gradual and increasing concentrations (70%, 90%, Absolute and Xylol) and were “embedded” in paraffin. The blocks were subjected to continuous cuts with a thickness of 5 µm using a microtome (SLEE, cut 6062) on silanized slides. The methodology for preparing

slides for immunohistochemistry was adapted from Bertolo [26]. The slides were rehydrated in alcoholic solutions with decreasing concentrations (Xylol, Absolute, 90% and 70%) and then the tissues were deparaffinized in an oven at 60ºC for one hour and, subsequently, hydrated again in alcoholic solutions with decreasing concentrations, as mentioned above, until washed in distilled water.

Immunohistochemical analysis for apoptosis was performed with rabbit anti-caspase-3 primary polyclonal antibody (Abcam, Code ab4051). Antigen recovery was performed by heat in a steam cooker (Philips Walita), with a citrate solution pH 6.0, for 40 minutes. Then, the slides were kept for 20 minutes at room temperature. After this period, endogenous peroxidase was blocked with a solution of methanol (Synth) and hydrogen peroxide (30 volumes, Synth) at 8%, for one hour, at room temperature and in a place protected from light. To block non-specific proteins, a commercial product (Protein Block, DakoCytomation, Code X0909) was used for one hour in a humid chamber at room temperature. Additionally, blocking was carried out with 8% skimmed milk powder (Molico, Nestlé), for one hour, in a dark humid chamber at room temperature. The primary antibody was incubated at a dilution of 1:200 for 18 h at 4º C. After that, the tissues were incubated with the peroxidase-linked polymer complex (Advance HRP kit, DakoCytomation, Code K4068). Between each of the steps described, baths were carried out in distilled water and in Tris HCl buffer solution, pH 7.4. To visualize the reaction, the chromogen DAB (3,3-diaminobenzidine – DakoCytomation, Code K3468-1) was used. The tissues were counterstained with Harris Hematoxylin and the mounting medium used was Entellan (Merck). As a positive control for the reaction, a dog lymph node was used. The negative control was performed with antibody diluent (DakoCytomation, Code S3022), replacing the primary antibody.

2.2.6.1. Morphometric Evaluation of Luteal Cells

The morphometric evaluation of luteal cells was performed from immunohistochemistry slides, using Image Pro Plus software (Media Cybernetics). The area (μm2) of 100 large luteal cells and 100 small luteal cells on each slide was analyzed [26].

2.2.6.2. Evaluation of caspase activity by pixel counting on immunohistochemistry slides

Immunohistochemistry slides were prepared containing six sections from each ovary, five quadrants were analyzed from each slide, totaling 30 fields. The slides were analyzed using an optical microscope (IX70, Olympus Corporation, Japan), using 40x magnification and quantification of pixels of immunostained cells carried out using Image Pro plus® software (version 1.51p) (Appendix 2), in which obtained the variables NVP (numeric value of pixels) and heterogeneity (standard deviation of NVP).

2.2.7. microRNAs Analysis

After slaughter, the remaining portion of the CLs were kept in cryotubes immersed in liquid nitrogen, for subsequent analysis of microRNAs at the Laboratory of Molecular Morphosiology and Development (LMMD) – University of São Paulo – Pirassununga – SP. Thirty-nine miRNAs were chosen for the present study (Appendix 1) based on their regulatory functions, such as angiogenesis, apoptotic pathways and recruitment of immune cells, in accordance with the literature. All protocols used in this experiment were carried out according to the manufacturer's instructions and described by Ferronato and collaborators (2023).

For extraction and purification of total RNA from CLs, 1mL of Trizol® reagent (Invitrogen, Carlsbad, United States) was used after maceration of the CLs. The separation phase occurred using 200µL of chloroform (Invitrogen, Carlsbad, United States) with centrifugation at 12,000xg at 4 °C for 15 minutes. RNA extractions from CL samples were performed using 700 µl of isopropyl alcohol with a first centrifugation of 12,000xg at 4°C for 30 minutes. Then, 1mL of 75% alcohol was added and a new centrifugation at 20,000xg for 5 minutes was performed. After centrifugation, the supernatant was discarded and the pellet was resuspended in distilled water for quality analysis. To analyze RNA quality and concentration, a spectrophotometer (NanoDrop™ One/OneC; Thermo Fisher Scientific, Maryland, United States) 260:280 was used. After analysis, the samples were treated with DNaseI (Invitrogen, Carlsbad, United States).

For reverse transcription, cDNA formation was obtained with the commercial miScript® RT kit (Qiagen, Hilden, Germany) with 10x miScript HiFlex

Buffer. The reactions were performed using 10µl, containing 200µg of total RNA, 2µl of 5xHiFlex Buffer, 1µl of the nucleic acid mix and 1µl of the reverse transcriptase enzyme. Transcription reactions were conducted using a thermocycler (ProFlex PCR System - Thermo Fisher Scientific, Maryland, United States), where it remained at 37°C for 60 minutes followed by an increase in temperature to 95°C for 5 minutes.

Reverse transcription analysis and quantification of miRNAs were performed with RT-PCR, which were performed with the miScript SYBR® Green commercial kit (Qiagen, Hilden, Germany). Reactions were performed with a total volume of 5 µl consisting of 3µl of QuantTect SYBR Green PCR Master mix, 0.6 µl of 10x miScript Universal Primer, 1.37 µl of RNAse water, 0.03 µl of 10x cDNA, and 1 µl of 10mM specific primers for the chosen miRNAs, previously used by Avila [27] (Appendix 1). Amplifications were performed using StudioTM 6 Flex equipment (Thermo Fisher Scientific, Maryland, United States). The reactions activating DNA polymerase were carried out with an initial incubation of 95°C/15 min and 45 cycles of 94°C/15', 55°C/30' and 70°C/30'. Amplification efficiency was evaluated based on CT and melting curve. Samples below the CT after 37 cycles were eliminated from analysis. Samples were normalized using the miR-99b CT and data were normalized by the formula 2--ΔCt ±SEM, as described by Ferronato [28]. The miRNAs were analyzed as present and absent within the dose variable groups (50% and 100%). The miRNAs that were exclusive to each group, that is, present in only one of them, were used to profile the miRNAs in each phase of the estrous cycle.

2.3. Statistical analysis

The design of Experiment 1 was completely randomized with a 2 (types of PGF) x 2 (doses) factorial arrangement with repeated measurements over time, in each phase of the estrous cycle (metestrus and diestrus). Fixed effects of type and dose of PGF2α, time after treatment administration, as well as interactions were included in the model.

Experiment 2 had the same design as Experiment 1, with measurements being repeated over time only for the progesterone variable. The main effects of PGF types and dose were considered in the model, as well as the interactions between these factors.

Breed, category, repetitions, animal and ECC were included as random effects for both experiments.

Data from both experiments are represented by the mean adjusted by LS Means ± standard error of the mean. ANOVA followed by Tukey's test (SAS Institute Inc., Cary, NC, USA) was used with significance at <0.5.

The miRNAs were analyzed as present and absent in each animal at the dose variable. The miRNA present in five or more samples in groups with 6 animals and present in 4 or more samples in groups with 5 animals was classified as present. MiRNAs that did not qualify as present were classified as absent. Exclusive miRNAs, that is, only present in one group, were used to outline the molecular profile of each phase of the estrous cycle according to the dose used.

3. Results

3.1. Experiment 1

3.1.1. Metestrus

P values of the main effects and interactions are shown in Table 1.

Table 1. P values for corpus luteum variables analyzed in Experiment 1, phase - metestrus, according to main effects and interactions.

Variables	PGF	Dose	Time	PGF*Dose	PGF*Time	Dose*Time	PGF*Dose*Time
Area (cm²)	0.05	**0.03**	**<.01**	0.51	0.94	0.64	0.99
VP (%)	0.09	**0.02**	0.047	0.71	0.61	0.36	0.36
Vascularization of CL	**0.01**	0.62	0.08	0.23	0.69	0.26	0.89
P4 (ng/ml)	0.35	**<.01**	0.046	0.54	0.99	0.14	0.87

Note: VP (vascular perfusion); P4 (serum progesterone)

In the ultrasonographic morphological variable of area, results of main effects of dose and time were obtained. Regarding dose effect, a smaller area was obtained when 100% of the recommended dose was used (Figure 1A). Concerning time effect, the area declined 48 hours after treatment administration, independent of drug and dose, remaining similar until 96h (Figure 1B).

Evaluating the percentage of vascular perfusion (VP%) using Doppler mode, a main effect of dose was also observed. A lower VP% was obtained when 100% of the recommended dose was used (Figure 2).

In the CL vascularization, a main effect of PGF2α was observed; a lower general vascularization of the CL was observed when DT was used, regardless of dose and time (Figure 3).

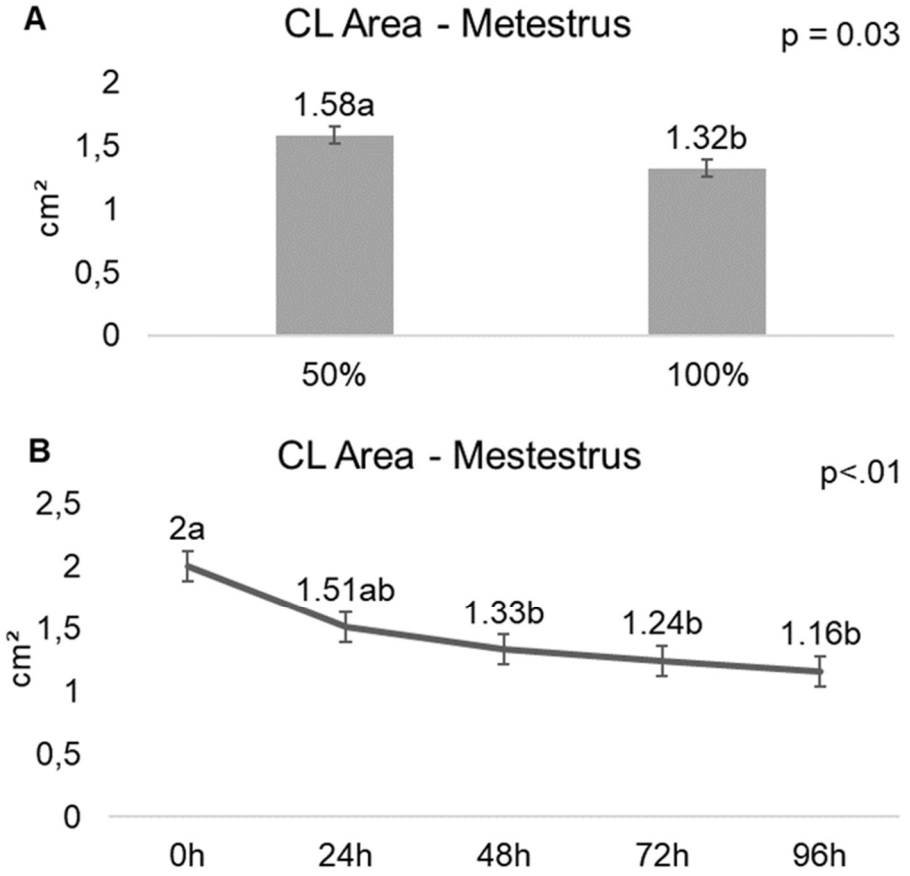

Figure 1. Area dynamics according to the main effect of dose (A) and time (B) in the metestrus phase. Values followed by different letters are significant (P < 0.05).

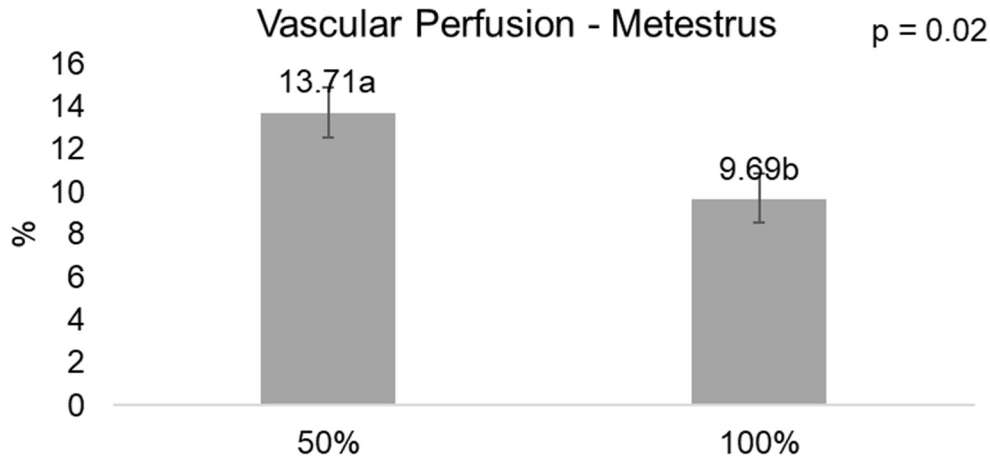

Figure 2. Effect of dose on the vascular perfusion variable; Values followed by different letters are significant (P= 0.02).

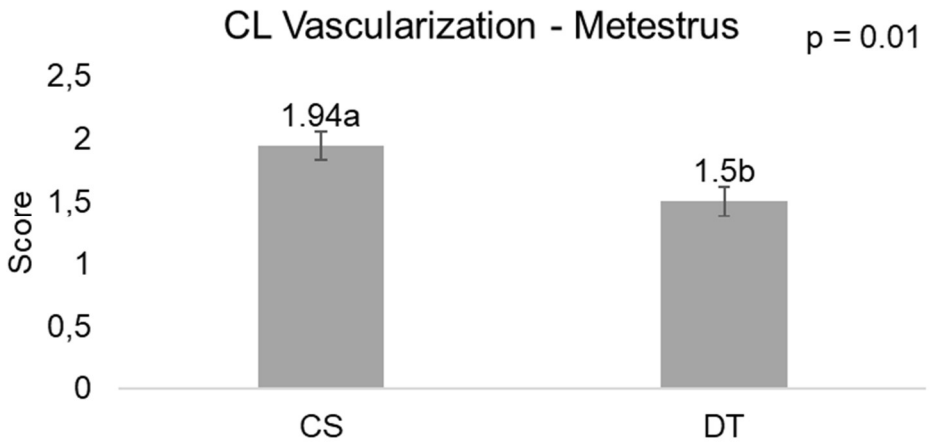

Figure 3. Dynamics of CL vascularization according to the main effect of PGF2α in the metestrus phase; Values followed by letters are significant (P = 0.01).

For progesterone levels, a dose effect was observed; when 100% of the recommended dose was used, lower serum progesterone levels were obtained (Figure 4A). Although not statistically significant, a numerical decline, (below 1ng/mL) in the first 48 hours was observed however returning to values above 1ng/mL after 96 hours (Figure 4B).

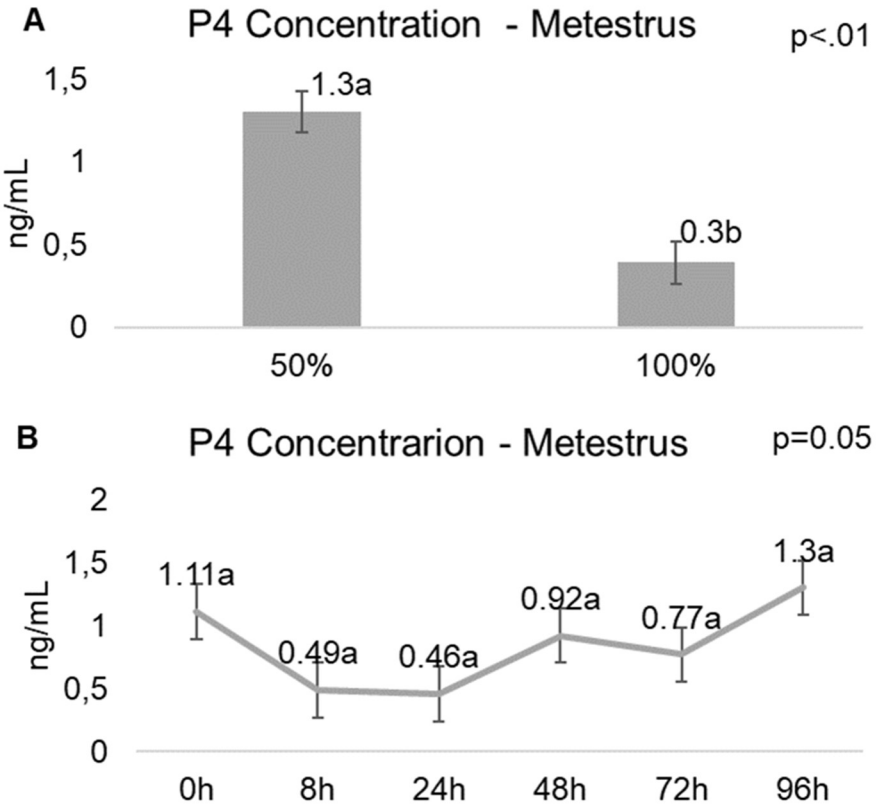

Figure 4. Dynamics of serum progesterone concentration according to the main effect of dose on the metestrus phase (A) and time (B); Values followed by different letters are significant (P < 0.05).

3.1.2. Diestrus

P values of the main effects and interactions are shown in Table 2.

Table 2. P values for corpus luteum variables analyzed in Experiment 1, phase - diestrus, according to main effects and interactions.

Variables	PGF	Dose	Time	PGF*Dose	PGF*Time	Dose*Time	PGF*Dose*Time
Area (cm^2)	0.43	0.13	**<.01**	0.25	0.86	0.96	0.95
VP (%)	0.41	0.77	**<.01**	0.12	0.86	0.3	0.22
Vascularization of CL	0.23	0.21	**<.01**	0.24	0.9	0.19	0.05
P4 (ng/ml)	0.85	0.41	**<.01**	0.57	0.92	0.58	0.87

Note: VP (vascular perfusion); P4 (serum progesterone)

The main effect of time occurred in all diestrus variables. Area declined from 24h to 96h (Figure 5A). The vascularization variables (VP% and CL vascularization) declined in the first 24h and 48h, maintaining similar values until 96h (Figure 5B and 5C, respectively).

In serum progesterone levels, a greater decline was also observed in the first 24 hours and remained constant until 96 hours (Figure 5D).

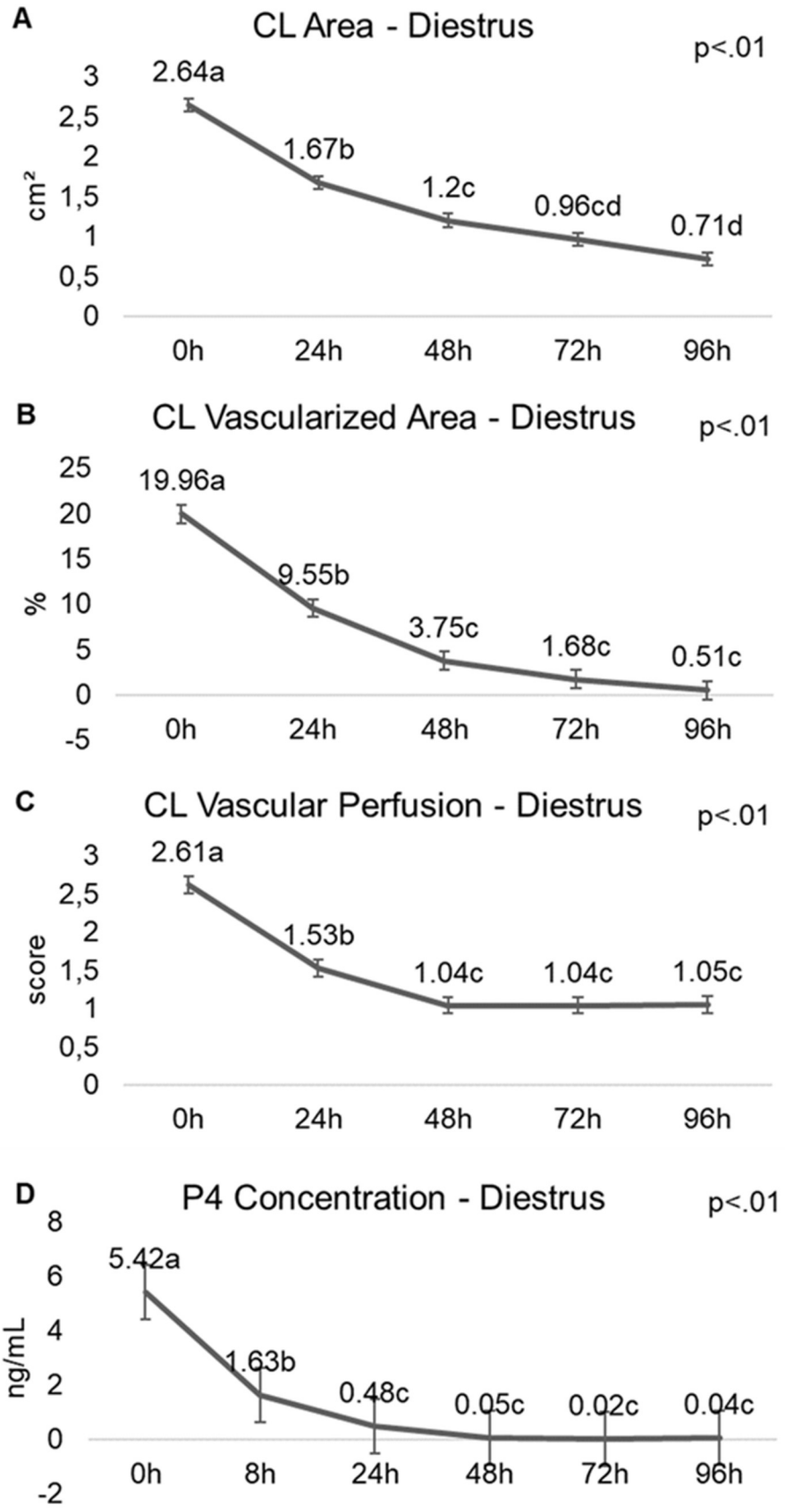

Figure 5. Dynamics of the area (A), vascularized area (B), CL vascularization (C) and serum progesterone (D) according to the main effect of time in the diestrus phase. Values followed by letters are significant (P < 0.01).

3.2. Experiment 2

3.2.1. Metestrus

The P values of the main effects and interactions are presented in Table 3.

Table 3. P values for each variable analyzed in Experiment 2 of metestrus, according to main effects and interactions.

Variables	PGF	Dose	Time	PGF*Dose	PGF*Time	Dose*Time	PGF*Dose*Time
P4 (ng/mL)	<.01	0.23	<.01	<.01	0.46	0.63	0.25
SLC Area	<.01	<.01	-	0.05	-	-	-
LLG Area	<.01	<.01	-	<.01	-	-	-
NVP	0.37	<.01	-	<.01	-	-	-
Heterogenity	0.43	<.01	-	<.01	-	-	-

Note: P4 (serum progesterone); SLC (small luteal cells); LLG (large luteal cells); NVP (numerical value of pixels).

In Experiment 2, during metestrus, there was also an interaction between dose*PGF2α, so that animals treated with DT50% obtained a higher level of serum progesterone, compared to all other treatments ($p<0.01$; Figure 6A). In this same variable, the main effect of time was significant for serum progesterone dosage, with a decline occurring between 0h and 24h ($p<0.01$; Figure 6B).

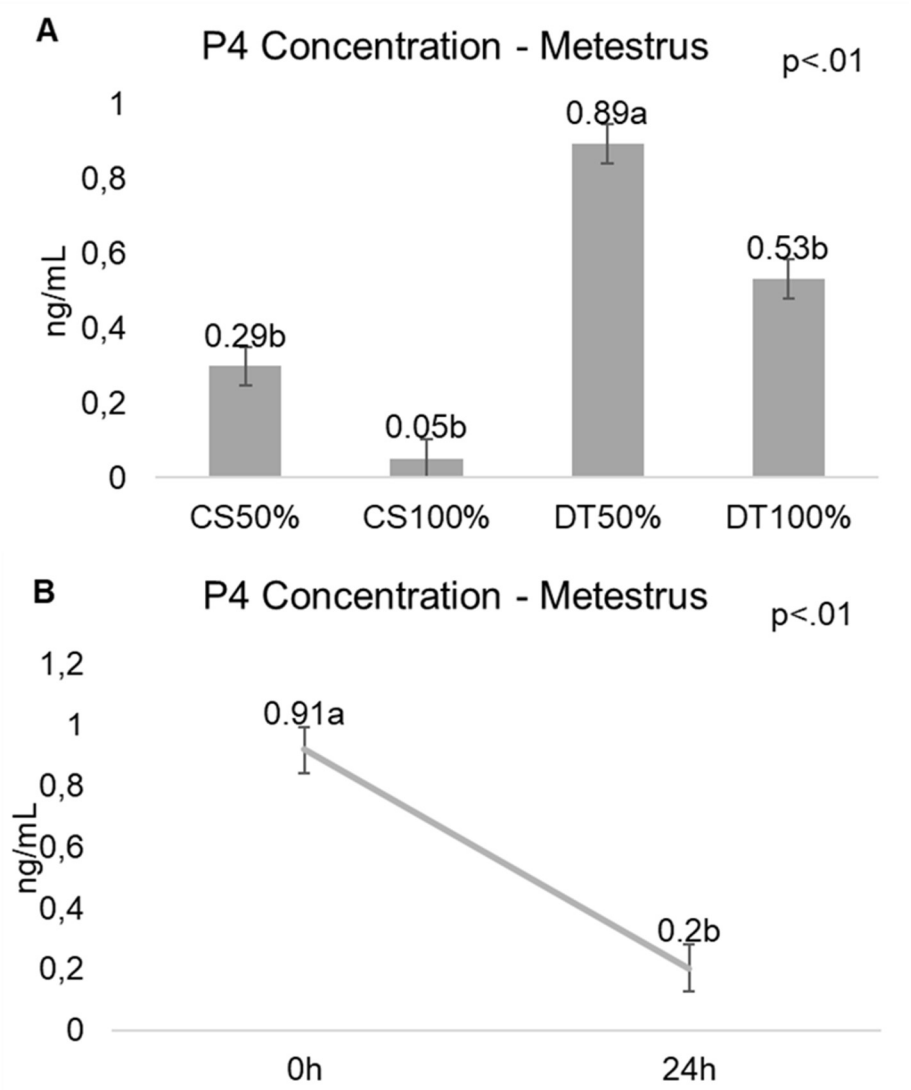

Figure 6. Dynamics of serum progesterone concentration according to dose interaction with PGF2α (CS50%: n=3, CS100%: n=3, DT50%: n=3, DT1005: n=3) (A) and to the main effect of time (A). Values followed by letters are significant (P < 0.01).

In the morphometry analysis, SLC was affected by dose and PGF, with the smallest areas found when using 50% (p<0.01; Figure 7A) of the dose and when using DT (p<0.01; Figure 7B). In LLC, an interaction between PGFα *dose was found, with a smaller area obtained after treatment with CS100% (p<0.01; Figure 7C).

For NVP, the lowest value occurred in the CS100% group, followed by DT50% and the highest value was in the CS50% group. The DT100% group did not differ from DT50% and CS100% (p<0.01; Figure 7D). With the heterogeneity variable, there was also an interaction between PGF2α*dose, all treatments were different from each other (p<0.05), the two extremes were found in DT, obtaining

higher values when 50% was used and lower values when 100% was administered (Figure 7E).

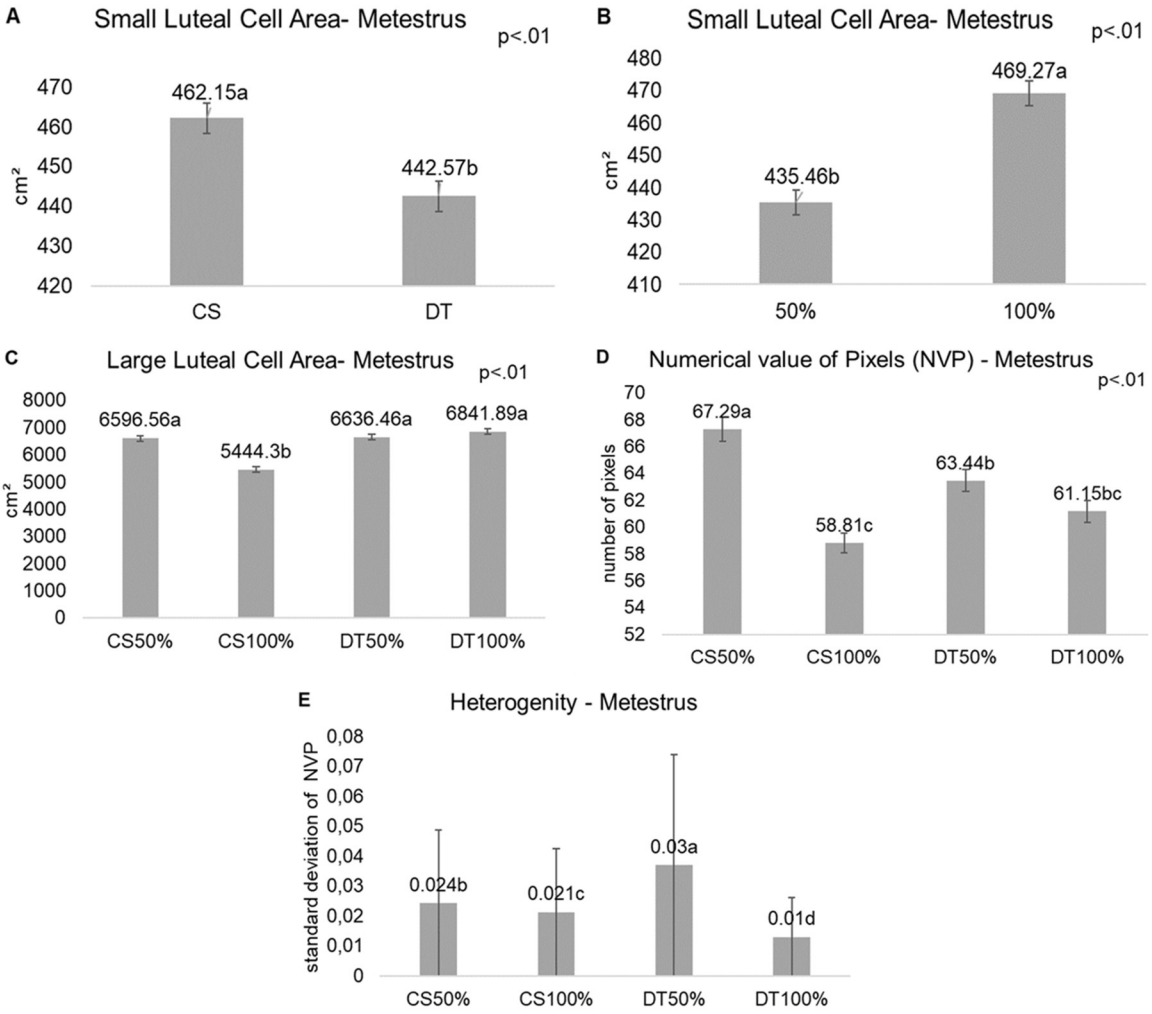

Figure 7. Plots of the main effect of PGF2α (A) and dose (B) on the SLC area variable; and interactions between dose and PGF2α in the variables of LLC area (C), NVP (D) and heterogeneity (D). N of groups: CS50%=3; CS100%=3; DT50%=3; DT100%=3. Values followed by differents letters are significant ($P < 0.05$).

3.2.2. Diestrus

The P values of the main effects and interactions are presented in Table 4.

Table 4. P values for each variable analyzed in Experiment 2 of diestrus, according to main effects and interactions.

Variables	PGF	Dose	Time	PGF*Dose	PGF*Time	Dose*Time	PGF*Dose*Time
P4 (ng/mL)	0.53	0.65	**<.01**	0.72	0.99	0.38	0.28
SLC Area	**<.01**	**<.01**	-	**<.01**	-	-	-
LLG Area	**<.01**	**0.03**	-	0.19	-	-	-
NVP	0.68	0.5	-	**0.02**	-	-	-
Heterogenity	**<.01**	0.21	-	0.83	-	-	-

Note: P4 (serum progesterone); SLC (small luteal cells); LLG (large luteal cells); NVP (numerical value of pixels).

During diestrus, there was a decline in P4 levels between 0h and 24h ($p<0.05$, Figure 8)

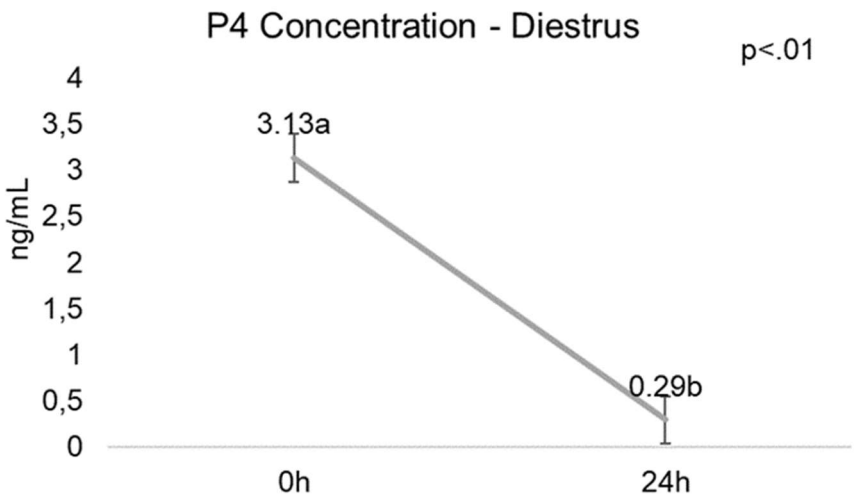

Figure 8. Dynamics of serum progesterone concentration according to the main effect of time in diestrus. Values followed by letters are significant ($P < 0.05$).

In the CL morphometry analysis, SLC showed an interaction between PGF2α and dose ($p<0.01$). A larger area was observed when the DT100% treatment was used, followed by CS50% and, finally, CS100% and DT50%, which did not differ from each other (Figure 9A). In LLC, two main effects were obtained, dose ($p= 0.03$) and PGF2α ($p<0.01$). A smaller area was obtained with CS compared to DT and, regarding the dose, this occurred when 50% of the recommended dose was used (Figure 9B and 9C).

In the NVP there was an interaction between PGF2α and dose ($p=0.02$), with the highest value found in the DT50% treatment, followed by CS100%, CS50% and, finally, the lowest value with the DT100% treatment (Figure 9D). In heterogeneity, only a difference regarding the type of PGF2α was obtained, with a greater heterogeneity value for CS ($p<0.01$, Figure 9E).

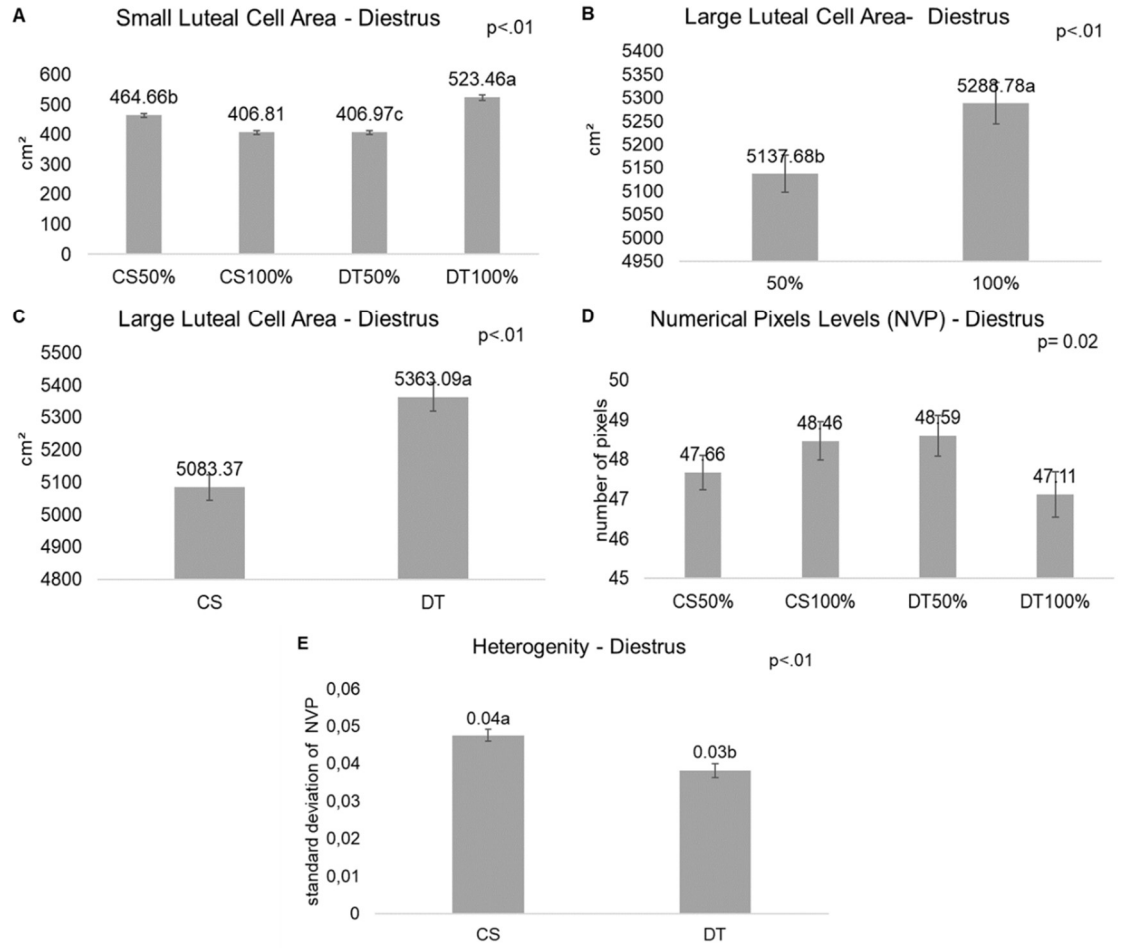

Figure 9. Interaction of PGF and dose on the CPL variables (A), main effect of PGF (B) and dose (C) on the LLC variable, interaction of PGF2α and dose on the number of pixels variable (D); and main effect of PGF on the heterogeneity variable (E). N of groups: CS50%=3; CS100%=3; DT50%=3; DT100%=2; 50%=6; 100%=5; CS=6 and DT=5; Values followed by lowercase letters are significant (P < 0.05).

Finally, the molecular profile regulating the process of luteolysis in this study is described below. Comparing the use of 50% of the dose in metestrus and diestrus, we obtained five miRNAs in common (bta-miR-132; bta-miR-143; bta-miR-125b; bta-miR-23a; bta-miR-120a) and 18 exclusive in the metestrus phase (bta-miR-145; bta-miR-182; bta-miR-183; bta-miR-202; bta-miR-378; bta-miR-let-7b; bta-miR-199- 3p; bta-miR-let-7e; bta-miR-let-7g; bta-miR-125a; bta-miR-126-5p; bta-miR-15a; bta-miR-17-5p; bta-miR-20a; bta-miR-26a; bta-miR-29a; bta-miR-34a; bta-miR-92a) (Figure 10A). However, when 100% of the recommended dose was used, 17 common miRNAs were found (bta-miR-143; bta-miR-183; bta-miR-202; bta-miR-let-7b; bta-miR-199- 3p; bta-miR-let-7e; bta-miR-let-7g; bta-miR-125a; bta-miR-125b; bta-miR-126-5p; bta-miR-23a; bta-miR-26a; bta-miR-29a; bta-miR-120a; bta-miR-34a; bta-miR-455-3p; bta-miR-

92a) and eight miRNAs exclusive to the diestrus phase (bta-miR-132; bta-miR-45; bta-miR-378; bta-miR-10b; bta-miR-15a; bta-miR-17-5p; bta-miR-181a; bta-miR-20a) (Figure 10B)

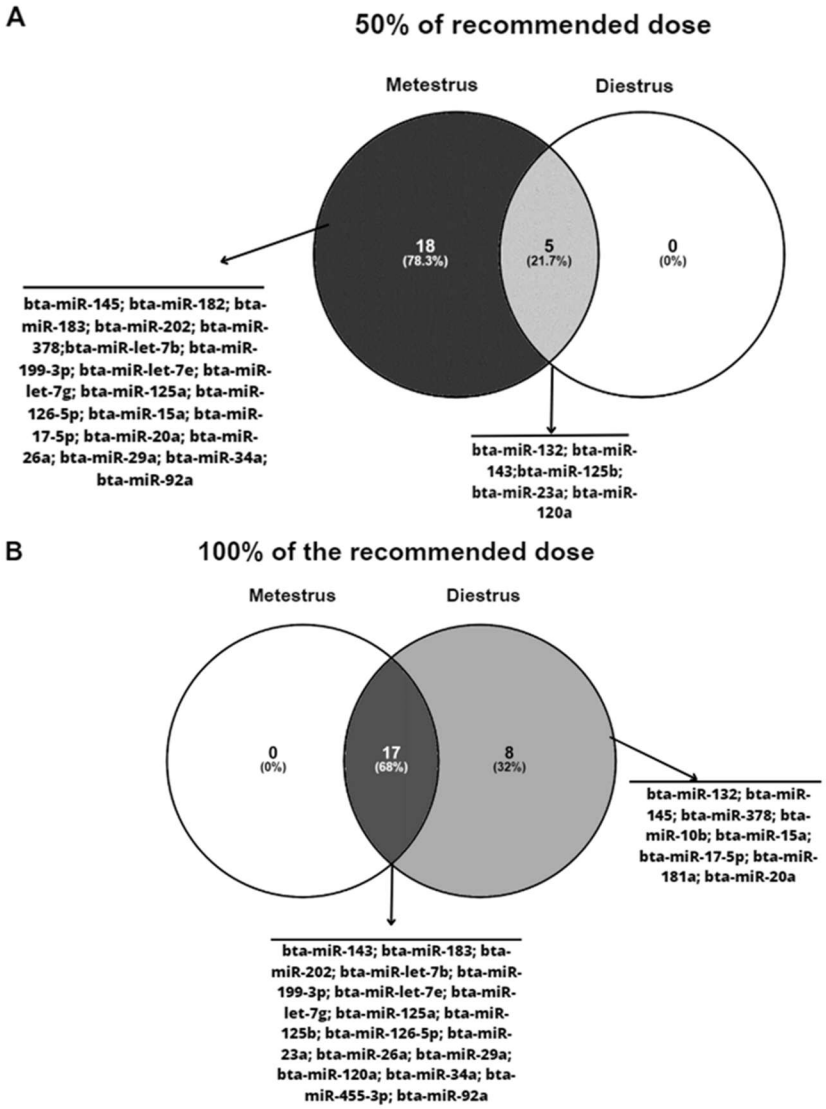

Figure 10. Venn diagram of exclusive and common miRNAs comparing metestrus and diestrus using doses 50% (A) and 100% (B) of the recommended dose.

Table 5. Summary of results.

METESTRUS	DIESTRUS
• **Exp1**	• **Exp1**
- CL Area: ↓ in the first 24h, values remaining until 96h. ↓ area when using 100% of the recommended dose.	**- CL Area:** ↓ constant in measurements until 72h, remaining low up to 96h, regardless of dose and PGFα .
-VP%: ↓ area when using 100% of the recommended dose.	**-VP%:** ↓ constant in measurements until 48h, remaining low up to 96h, regardless of dose and PGFα
-Vascularization of CL: ↓ When DT was used.	**- Vascularization of CL:** ↓ constant in measurements until 48h, remaining low up to 96h, regardless of dose and PGFα
-P4: ↓ concentration when 100% of the recommended dose was used	**-P4:** ↓ constant in measurements until 48h, remaining low up to 96h, regardless of dose and PGFα
• **Exp2**	• **Exp2**
-P4: Main effect time: ↓ independent of dose and PGFα. Dose*PGFα: highest [P4] with DT50%, followed by other treatments with similar values.	**-P4:** ↓ with 24h
-SLC Area: ↓ area with 50% of dose and DT.	**- SLC Area:** ↓ area with CS100% e DT50%, followed by CS50% and DT100%.
-LLC Area: ↓ area with CS50%.	**- SLC Area:** ↓ area with 50% of dose and CS.
-NVP: ↑ with CS50%, followed by other treatments with similar values	**-NVP:** ↓ value with DT100%, followed by CS50%, CS100% and finally DT50%.
-Heterogenity: ↑ DT50%, followed by CS50% and CS100%, and finally, DT100%	**- Heterogenity:** ↑ with CS.

Source: Trevisoli, 2023.

4. DISCUSSION

4.1. Metestrus

In the present study, in the metestrus phase, partial luteolysis was observed due to the decline in progesterone levels, below 1ng/mL, with a subsequent return of steroidoigenic functions, corroborating other studies in taurine[9,10] and zebu [29] females.

In morphological assessments, smaller dimensions were observed after 24 hours. It was also observed that when 100% of the recommended dose was used, there was a greater decline in CL area and blood perfusion. CL vascularization was lower when DT was used, regardless of the dose. Similar to the result with SLC morphometry, obtaining smaller areas using DT and 50% of the recommended dose.

Treatment with CS100% resulted in a greater decrease in serum P4 levels in Exp2., in the size of LLC and lower NVP. This indicates the activation of the luteolytic process. DT50% resulted in greater results in heterogeneity.

In the morphological analysis, it was possible to observe a decrease in luteal dimensions in ultrasound assessments of the CL after 24 hours and when 100% of the recommended dose was used. These results do not corroborate to those found by Acosta and collaborators [13], who did not find a reduction in area in the initial CL after administration of PGF2α at metestrus. Nevertheless, our results indicate a reduction in blood perfusion associated to the drop in P4 observed during metestrus when 100% of the PGF2α dose was used.

Although P4 concentrations had a slight decline in the first 24 hours regardless of the dose and PGF2α was used, a biological effect could be observed, as concentrations declined below 1 ng/mL after 8h, but exceeded this threshold after 96h, suggesting partial luteolysis. Similar results were obtained by Ferraz Junior. [30] and Nascimento [9] with the use of PGF2α in metestrus, who observed a process of partial luteolysis, with a drop in serum progesterone levels in the first 24 hours, returning its production from 96h.

In Exp.2 there was a reduction in serum P4 levels within 24 hours, however, as the samples were not collected after 24 hours, the effect of partial luteolysis could not be confirmed. Still in Exp.2, it was possible to observe that,

regardless of the moment, the drug x dose that caused the smallest decline in P4 was DT50% in relation to all other treatments.

In the area of small luteal cells, we can observe that smaller areas were found when using 50% of the dose and prostaglandin DT, inversely to what happened with LLC, where the smallest areas were when using CS100% treatment. This difference in drug action on each type of luteal cell may be due to the greater presence of PGF2α receptors on large luteal cells than on small ones [3,31].

In the numerical value of pixels, higher values could be observed with CS50%, indicating a lower luteolytic response, contrary to the CS100% group, which presented the lowest NVP. The different response of different drugs and doses does not corroborate the results of Korzekwa [32] who, through in vitro culture of luteal cells, obtained similarity between CS and DT in the expression of caspase-3. Regarding heterogeneity, Siqueira [33] obtained higher values at moments of CL formation and at the end of the cycle, with a more homogeneous result in the diestrus phase. In the present study, the DT50% treatment was the one with the greatest heterogeneity compared to the other groups, possibly indicating a greater luteolytic response [34].

4.2. Diestrus

In the present study, it was demonstrated that the use of 50% of the recommended dose guaranteed results similar to the use of 100% of the dose in the Exp.1 variables. This fact demonstrates that the use of half the dose of sodium cloprostenol (250 µg) or dinoprost tromethamine (12.5 mg) can be an effective alternative to induce luteolysis in responsive phases of CL in beef cattle. In the morphological results, when DT was used and 100% of the dose, a smaller area of the LLC was obtained. For the NVP variable, DT100% promoted better results and for heterogeneity this occurred with CS, regardless of the dose.

Ultrasonographic assessments of area, vascularization and blood perfusion of the CL of animals treated during diestrus, as well as serum P4 (Exp1) levels remained constant up to 96h, regardless of the dose and prostaglandin used. This differs from the results found by Ferraz Junior [30] in which 50% of the DT dose during diestrus did not show luteolytic efficiency in all animals. However, the present study corroborates several other studies that demonstrated that

reducing the doses of luteolytic agents to 50% of the recommended dose is an effective option for luteolytic induction in responsive phases of both taurine and zebu bovine females [35–37].

The findings in the present study corroborate part of what is available in the literature about reducing doses of different active ingredients of PGF2α during the diestrus phase. Analyzing the variable of serum P4 levels, we can observe that in both Exp1 and Exp 2 there was a drastic decline in the first 24 hours, remaining with concentrations below 1ng/mL, which corresponds to the luteolysis process and is in accordance with studies in sheep [38] and cattle [39–41]. There was no difference between the drugs, a result that differs from those obtained by Sedó et al. [42] with taurine heifers when using CS. They observed lower concentrations of P4 between 18 and 36h, compared to treatment with DT. In Exp 2, measurements were taken just 24 hours after the administration of PGF2α, however, when we observed the results of Exp 1, in which there are measurements up to 96 hours, it was possible to notice the occurrence of total regression of the steroidoigenic capacity and the beginning of structural luteolysis process, independent of drug and dose.

In addition to the functional luteolysis observed previously, results obtained also corroborate structural luteolysis, which is caused by cell death, apoptosis and cellular matrix remodeling [43,44]. Microscopically, observing the SLC, the smallest areas were obtained with CS100% and DT50%, a result that differs from that found by Choudhary and collaborators [45], who observed a greater reduction in the size of the SLC with increasing PGF concentration in *in vitro* culture. When we observed the LLC, we obtained a smaller area using the CS and also with 50% of the dose. We can find a similar methodology in the study by Trevisol and collaborators [46] which used underdosing (1/6 of the recommended dose - 83.3µg) and the double the recommended dose (500 µg) of CS in the initial diestrus. LLC analysis was carried out 24 and 40 hours after application of the drug. In this experiment, after the administration of the underdosage, there was a reduction in the expression of VEGFA mRNA after 24 hours of the administration, a drop in serum progesterone concentrations and a reduction in the size of the CL due to the reduction in the size of the LLC. This differs from that found by these authors when double the dose was used, whose results of VEGFA, Star and Fas-L mRNA expression, LLC size and serum

concentrations of P4 were corresponding to total luteolysis. We can assume that, in the present study, we obtained results of total luteolysis even with 50% of the dose and a more efficient reduction when the CS drug was used.

Furthermore, in pixel analysis, the best result found in NVP was using DT100%. As for the heterogeneity analysis, the best result, with greater heterogeneity, was using the drug cloprostenol, regardless of the dose. This result also differs from that found by Korzekwa [47]. Carambula and colleagues [34] observed increased expression of caspase-3 associated with structural luteolysis in sheep, proving the increase in caspase-3 as a luteolytic mediator. Peluffo and collaborators [48] were also able to observe that there is a physiological increase in caspase-3 with the maturation of the CL, that is, in the diestrus phase, similar to the present study.

With the morphofunctional results reported above, it was possible to observe that the use of 50% of the dose in metestrus does not cause luteolysis, unlike the diestrus phase in which 50% of the recommended dose promoted total luteolysis. This difference also occurred molecularly. In diestrus, no exclusive miRNA was found, while in metestrus, 18 exclusive miRNAs were found. Some of these have already been described in processes of granulosa cell apoptosis [18,49], angiogenesis, steroidogenesis [50] and immune cell recruitment [51]. With the use of the full dose (100% of the recommended dose) we obtained results corresponding to partial luteolysis in metestrus and total luteolysis in diestrus. We can also suggest that molecularly, the regulated pathways are distinct, due to the absence of exclusive miRNAs in metestrus and the presence of 8 exclusive miRNAs in the diestrus phase. Among these exclusive to diestrus, some functions related to cell apoptosis [49,52] and recruitment of immune cells [53] have been described.

In summary, the present study presents comprehensive data on the morphophysiological and molecular changes in the luteolysis induction process at the metestrus and diestrus. Future studies are needed in an attempt to further elucidate the luteolysis process.

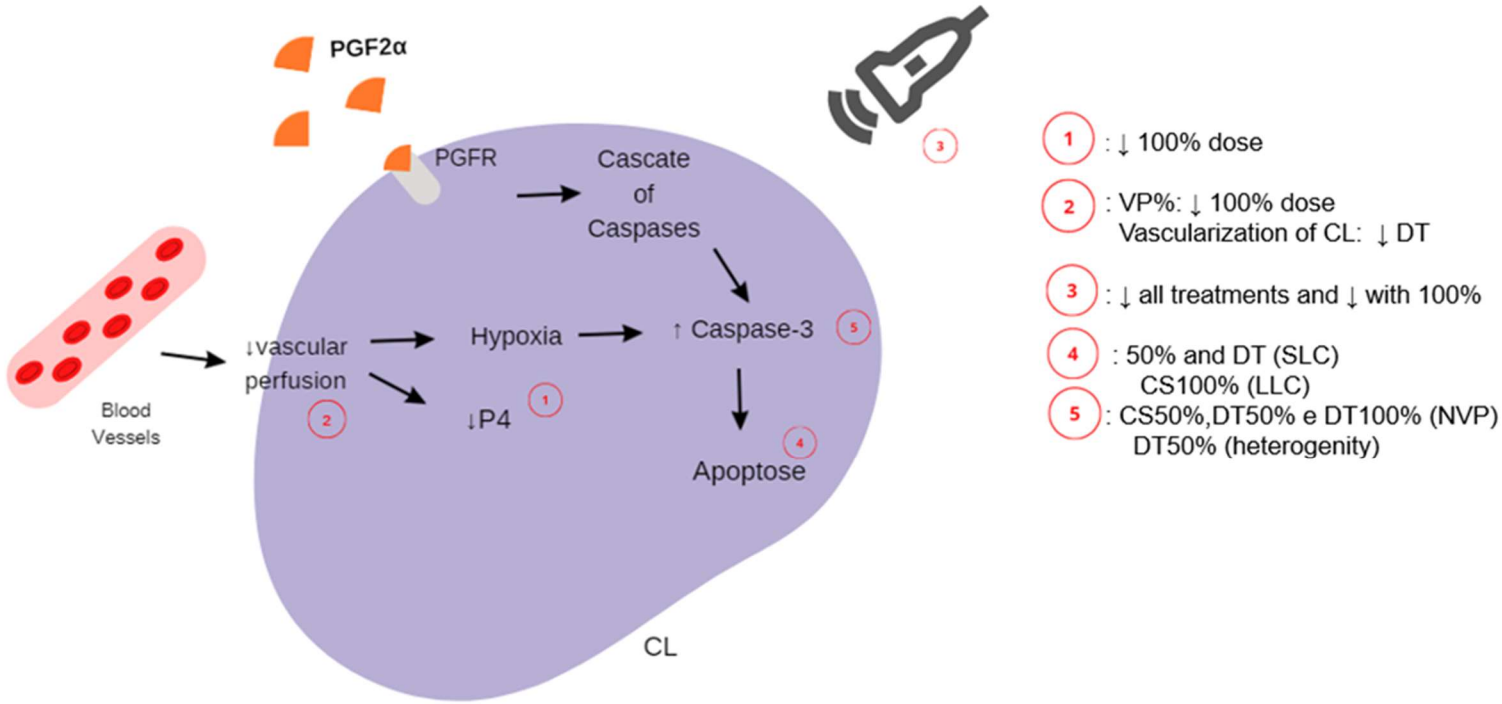

Figure 11. Representative scheme of luteolysis after binding of PGF2α to the receptor in luteal cells in the metestrus phase. The numbers represent the variables analyzed in the present study (1- serum progesterone dosage; 2- vascular analysis by Doppler (VA: % of vascular perfusion and vascularization of the CL); 3- ultrasound morphometry analysis; 4- morphometry analysis of SLC (small lutein cells) and LLC (large lutein cells); 5- caspase-3 immunostaining evaluated by pixels (NVP: numerical value of pixels and heterogeneity: standard deviation of NVP). The symbols present in the image represent: (↓) - decline; The numerical markings represent the active location of each variable. The legend shows the drug or dose that had the best luteolytic response. CS50%: 50% of the recommended dose of cloprostenol sodium; CS100%: 100% of the recommended dose of cloprostenol sodium; DT50%: 50% of the recommended dose of dinoprost tromethamine, DT100%: 100% of the dose of dinoprost tromethamine.

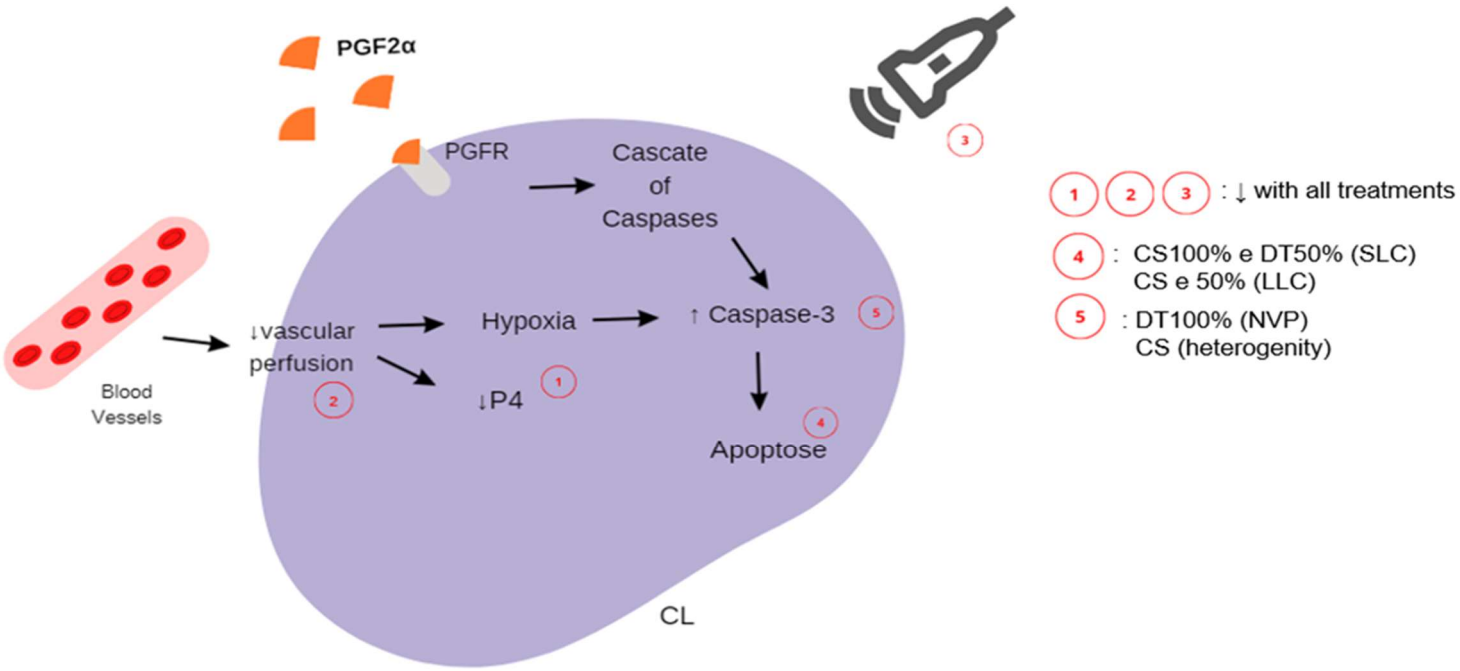

Figure 12. Representative scheme of luteolysis after binding of PGF2α to the receptor in luteal cells in the diestrus phase. The numbers represent the variables analyzed in the present study (1- serum progesterone dosage; 2- vascular analysis by doppler (VP: vascular perfusion and vascularization of the CL); 3- ultrasound morphometry analysis; 4- morphometry analysis of SLC (small lutein cells) and LLC (large lutein cells); 5- caspase-3 immunostaining evaluated by pixels (NVP: numerical value of pixels and heterogeneity: standard deviation of NVP). The symbols present in the image represent: (↓) - decline; The numerical markings represent the active location of each variable. The legend shows the drug or dose that had the best luteolytic response. CS50%: 50% of the recommended dose of cloprostenol sodium; CS100%: 100% of the recommended dose of cloprostenol sodium; DT50%: 50% of the recommended dose of dinoprost tromethamine, DT100%: 100% of the dose of dinoprost tromethamine.

5. CONCLUSIONS

At metestrus, the phenomenon of partial luteolysis could be observed regardless of the dose or PGF2α, despite showing a smaller CL area and perfusion when 100% of the dose was used. Less vascularization of the CL and size of the SLC could be observed when DT was used.

During diestrus, it was possible to observe total regression using 50% or 100% of the recommended dose regardless of the PGF2α used, however the CS had better results lowering pixel count (NVP) and the DT in reducing LLC. It is not possible to highlight a more effective PGF2α in the luteolysis process.

It is assumed that miRNAs act throughout the luteolysis process, being able to modulate steroid production genes, up to the activation of pro-apoptotic pathways. Future studies are needed to provide in-depth detail on the luteolytic pathways in cattle.

6. FINANCING DECLARATION

This study was funded by the Coordination for the Improvement of Higher Education Personnel – Brazil (CAPES, Financial Code 001) and by the Postgraduate Program in Veterinary Medicine of the Faculty of Agricultural and Veterinary Sciences (FCAV-UNESP).

7. DECLARATION OF COMPETITION INTEREST

The authors declare no conflicts of interest.

8. ACKNOWDGEMETNS

The authors would like to thank Ourofino Saúde Animal for all the assistance provided during the development of the study.

9. AUTHORS' CONTRIBUTION

Marina Marina Anchieta Trevisoli: Conceptualization; Investigation; Methodology; Data analysis; Essay; Review and Editing;

Gabriel Artur Marciano do Nascimento: Conceptualization; Investigation; Methodology; Data analysis; Essay; Review and Editing;

Lindsay Unno Gimenes: Conceptualization; Methodology; Review and Editing; Financial resources

Ana Clara Degan Mattos: Investigation; Methodology; Data analysis

Rosemeri by Oliveria Vasconcelos: Methodology

Paulo Henrique Leal Bertolo: Methodology

Vanessa Garcia Rizzi Mussi: Methodology

Rafael Rodrigues Corrêa: Methodology

Cláudia Cristina Paro de Paz: Statistical Analysis

Guilherme Paula Nogueira: Methodology;

Natália Marins Bastos: Methodology and statistical analysis;

Juliano Correa da Silveira: Methodology and Review.

All authors critically reviewed the manuscript and approved the final version.

10. REFERENCES

[1] Sartori R, Haughian JM, Shaver RD, Rosa GJM, Wiltbank MC. Comparison of ovarian function and circulating steroids in estrous cycles of Holstein heifers and lactating cows. J Dairy Sci 2004;87:905–20. https://doi.org/10.3168/jds.S0022-0302(04)73235-X.

[2] Mccracken JA, Custer EE, Lamsa JC. Luteolysis: A neuroendocrine-mediated event. Physiol Rev 1999;79:263–323. https://doi.org/10.1152/physrev.1999.79.2.263.

[3] Stocco C, Telleria C, Gibori G. The molecular control of corpus luteum formation, function, and regression. Endocr Rev 2007;28:117–49. https://doi.org/10.1210/er.2006-0022.

[4] Donaldson LE. A comparison of cloprostenol and dinoprost tromethamine for the control of estrus in bovine embryo transfer. Theriogenology 1984;21:1019–22. https://doi.org/10.1016/0093-691X(84)90397-2.

[5] Etherington WG, Kelton DF, Adams JE. Reproductive performance of dairy cows following treatment with fenprostalene, dinoprost, or cloprostenol between 24 and 31 Days post partum: A field trial. Theriogenology 1994;42:739–52. https://doi.org/10.1016/0093-691X(94)90442-L.

[6] Salverson RR, DeJarnette JM, Marshall CE, Wallace RA. Synchronization of estrus in virgin beef heifers using melengestrol acetate and PGF2α: an efficacy comparison of cloprostenol and dinoprost tromethamine. Theriogenology 2002;57:853–8. https://doi.org/10.1016/S0093-691X(01)00692-6.

[7] Pursley JR, Martins JPN, Wright C, Stewart ND. Compared to dinoprost tromethamine, cloprostenol sodium increased rates of estrus detection, conception and pregnancy in lactating dairy cows on a large commercial

dairy. Theriogenology 2012;78:823–9. https://doi.org/10.1016/J.THERIOGENOLOGY.2012.03.032.

[8] Stevenson JS, Phatak AP. Rates of luteolysis and pregnancy in dairy cows after treatment with cloprostenol or dinoprost. Theriogenology 2010;73:1127–38. https://doi.org/10.1016/j.theriogenology.2010.01.014.

[9] Nascimento AB, Souza AH, Keskin A, Sartori R, Wiltbank MC. Lack of complete regression of the Day 5 corpus luteum after one or two doses of PGF2α in nonlactating Holstein cows. Theriogenology 2014;81:389–95. https://doi.org/10.1016/j.theriogenology.2013.10.009.

[10] Trevisol E, Ferreira JC, Ackermann CL, Destro FC, Marques Filho WC, Carmagos AS, et al. Luteal changes after treatment with sub-luteolytic doses of prostaglandin (cloprostenol sodium) in cattle. Anim Reprod Sci 2015;153:8–12. https://doi.org/10.1016/j.anireprosci.2014.12.005.

[11] Tsai S-J, Wiltbank MC. Prostaglandin F2α Regulates Distinct Physiological Changes in Early and Mid-Cycle Bovine Corpora Lutea1. Biol Reprod 1998;58:346–52. https://doi.org/10.1095/biolreprod58.2.346.

[12] Diaz FJ, Anderson LE, Wu YL, Rabot A, Tsai SJ, Wiltbank MC. Regulation of progesterone and prostaglandin F2α production in the CL. Mol Cell Endocrinol 2002;191:65–80. https://doi.org/10.1016/S0303-7207(02)00056-4.

[13] Acosta TJ, Yoshizawa N, Ohtani M, Miyamoto A. Local changes in blood flow within the early and midcycle corpus luteum after prostaglandin F(2 alpha) injection in the cow. Biol Reprod 2002;66:651–8. https://doi.org/10.1095/BIOLREPROD66.3.651.

[14] Trevisol E, Ferreira JCP, Ackermann CL, Destro FC, Amaral JB. Luteólise em bovinos: revisão Luteolysis in cattle: review. n.d.

[15] Martin SJ. Caspases: Executioners of Apoptosis. Pathobiol Hum Dis A Dyn Encycl Dis Mech 2014;16:145–52. https://doi.org/10.1016/B978-0-12-386456-7.01411-8.

[16] Grivicich I, Regner A, da Rocha AB. Morte Celular por Apoptose. Rev Bras Cancrol 2007;53:335–43. https://doi.org/10.1590/S0102-311X2003000200031.

[17] Hossain M, Ghanem N, Hoelker M, Rings F, Phatsara C, Tholen E, et al. Identification and characterization of miRNAs expressed in the bovine ovary. BMC Genomics 2009;10:443. https://doi.org/10.1186/1471-2164-10-443.

[18] Gecaj RM, Schanzenbach CI, Kirchner B, Pfaffl MW, Riedmaier I, Tweedie-Cullen RY, et al. The dynamics of microRNA transcriptome in bovine corpus luteum during its formation, function, and regression. Front Genet 2017;8:213. https://doi.org/10.3389/fgene.2017.00213.

[19] Bartel DP. MicroRNAs: Genomics, Biogenesis, Mechanism, and Function. Cell 2004;116:281–97. https://doi.org/10.1016/S0092-8674(04)00045-5.

[20] Maalouf SW, Smith CL, Pate JL. Changes in microRNA expression during maturation of the bovine corpus luteum: Regulation of luteal cell proliferation and function by microRNA-34a. Biol Reprod 2016;94. https://doi.org/10.1095/biolreprod.115.135053.

[21] Xu MQ, Jiang H, Zhang LQ, Sun XL, Luo D, Fu Y, et al. MiR-29b affects the secretion of PROG and promotes the proliferation of bovine corpus luteum cells. PLoS One 2018;13. https://doi.org/10.1371/journal.pone.0195562.

[22] Ma T, Jiang H, Gao Y, Zhao Y, Dai L, Xiong Q, et al. Microarray analysis of differentially expressed microRNAs in non-regressed and regressed bovine corpus luteum tissue; microRNA-378 may suppress luteal cell apoptosis by targeting the interferon gamma receptor 1 gene. J Appl Genet 2011;52:481–6. https://doi.org/10.1007/s13353-011-0055-z.

[23] De Jaboticabal C, Veterinário M. "AVALIAÇÃO DA EFICIÊNCIA LUTEOLÍTICA DE DIFERENTES DOSES DE CLOPROSTENOL SÓDICO E DINOPROST TROMETAMINA ADMINISTRADAS NOS DIAS 4 E 11 DO CICLO ESTRAL DE FÊMEAS BOVINAS DE CORTE" Gabriel Artur Marciano do Nascimento. Universidade Estadual Paulista (UNESP); 2019.

[24] Cachapuz JMS. Experiencias com o desmame aos 60 e 90 dias. Emater 1997:1–52.

[25] Pugliesi G, Rezende RG, Silva JCB da, Lopes E, Nishimura TK, Baruselli PS, et al. Use of Doppler ultrasonography in timed-AI and ET programs in cattle. / Uso da ultrassonografia Doppler em programas de IATF e TETF em bovinos. Rev Bras Reprodução Anim 2017;41:140–50.

[26] Bertolo P, … PM-J of, 2019 undefined. Immunodetection of Leishmania infantum in the subungual área of dogs with visceral leishmaniasis. Doencas-Parasitarias-Dos-Animais … n.d.

[27] de Ávila A, Bridi A, Andrade G, Del Collado M, Sangalli J, Nociti R, et al. Estrous cycle impacts miRNA content in extracellular vesicles that modulate bovine cumulus cell transcripts during in vitro maturation Running title: Effect of different estrous cycle on small EVs. Biol Reprod 2019.

[28] de Ferronato GA, Cerezetti MB, Bridi A, Prado CM, Dos Santos G, Bastos NM, da Rosa PMS, Ferst JG da SJ. MicroRNA Profiling Using a PCR-Based Method. Methods Mol Biol., 2023, p. 2595:159-170. https://doi.org/10.1007/978-1-0716-2823-2_11.

[29] Ferraz Junior MVC, Pires A V., Biehl MV, Santos MH, Polizel DM, Nepomuceno DD, et al. Luteolysis in Bos indicus cows on Days 5 and 7 of estrous cycle with varying doses of PGF2α. Theriogenology 2016;86:1268–74. https://doi.org/10.1016/j.theriogenology.2016.04.067.

[30] Ferraz Junior MVC, Pires A V., Biehl MV, Santos MH, Polizel DM, Nepomuceno DD, et al. Luteolysis in Bos indicus cows on Days 5 and 7 of estrous cycle with varying doses of PGF2α. Theriogenology 2016;86:1268–74. https://doi.org/10.1016/j.theriogenology.2016.04.067.

[31] Wiltbank MC. Cell types and hormonal mechanisms associated with mid-cycle corpus luteum function. J Anim Sci 1994;72:1873–83. https://doi.org/10.2527/1994.7271873x.

[32] Korzekwa AJ, Okuda K, Woclawek-Potocka I, Murakami S, Skarzynski DJ. Nitric oxide induces apoptosis in bovine luteal cells. J Reprod Dev 2006;52:353–61. https://doi.org/10.1262/jrd.17092.

[33] Siqueira LGB, Torres CAA, Amorim LS, Souza ED, Camargo LSA, Fernandes CAC, et al. Interrelationships among morphology, echotexture, and function of the bovine corpus luteum during the estrous cycle. Anim Reprod Sci 2009;115:18–28. https://doi.org/10.1016/j.anireprosci.2008.11.009.

[34] Carambula SF, Matikainen T, Lynch MP, Flavell RA, Dias Gonçalves PB, Tilly JL, et al. Caspase-3 is a pivotal mediator of apoptosis during regression of the ovarian corpus luteum. Endocrinology 2002;143:1495–501. https://doi.org/10.1210/endo.143.4.8726.

[35] Granados-Villarreal LM, Zarco L, Mejía O, Sánchez-Torres MT, Pablos-Hach JL. Luteolytic efficiency of reduced doses of cloprostenol in the ewe. Effect of progesterone concentrations at the time of treatment. Anim Reprod Sci 2017;186:68–76. https://doi.org/10.1016/J.ANIREPROSCI.2017.09.006.

[36] Colazo MG, Martinez M, Kastelic JP, Mapletoft RJ, Colazo MG, Fabian Martínez M, et al. Effects of dose and route of administration of cloprostenol on luteolysis, estrus and ovulation in beef heifers. Elsevier 2002;72:47–62. https://doi.org/10.1016/S0378-4320(02)00087-8.

[37] Ginther OJ, Silva LA, Araujo RR, Beg MA. Temporal associations among pulses of 13,14-dihydro-15-keto-PGF 2alpha, luteal blood flow, and luteolysis in cattle. Biol Reprod 2007;76:506–13. https://doi.org/10.1095/biolreprod.106.057653.

[38] EL-Sherry TM, Senosy W, Mahmoud GB, Wasfy SI. Effect of dinoprost and cloprostenol on serum nitric oxide and corpus luteum blood flow during luteolysis in ewes. Theriogenology 2013;80:513–8. https://doi.org/10.1016/j.theriogenology.2013.05.007.

[39] Ginther OJ, Fuenzalida MJ, Shrestha HK, Beg MA. Concomitance of luteinizing hormone and progesterone oscillations during the transition from preluteolysis to luteolysis in cattle. DAE 2011;40:77–86. https://doi.org/10.1016/j.domaniend.2010.09.002.

[40] Martins J, Policelli R, Neuder L, … WR-J of dairy, 2011 undefined. Effects of cloprostenol sodium at final prostaglandin F2α of Ovsynch on complete luteolysis and pregnancy per artificial insemination in lactating dairy cows. Elsevier n.d.

[41] Meira C, Pessoa VM, Ferreira JCP, Araujo GHM, Gioso MM, Bicudo SD, et al. Alternative low doses and routes of administering a prostaglandin F2α analogue to induce luteolysis in Nelore cows. J Vet Sci 2006;7:387–90.

https://doi.org/10.4142/jvs.2006.7.4.387.

[42] Umaña Sedó SG, Figueiredo CC, Gonzalez TD, Duarte GA, Ugarte Marin MB, Crawford CA, et al. Evaluation of luteolysis, follicle size, and time to ovulation in Holstein heifers treated with two different analogs and doses of prostaglandin-F2α. J Dairy Sci 2022;105:5506–18. https://doi.org/10.3168/jds.2021-21487.

[43] Niswender GD, Juengel JL, Silva PJ, Rollyson MK, McIntush EW. Mechanisms controlling the function and life span of the corpus luteum. Physiol Rev 2000;80:1–29. https://doi.org/10.1152/physrev.2000.80.1.1.

[44] Bowolaksono A, Nishimura R, Hojo T, Sakumoto R, Acosta TJ, Okuda K. Anti-apoptotic roles of prostaglandin E2 and F2alpha in bovine luteal steroidogenic cells. Biol Reprod 2008;79:310–7. https://doi.org/10.1095/biolreprod.107.066084.

[45] Choudhary E, Sen A, Inskeep EK, Flores JA. Developmental sensitivity of the bovine corpus luteum to prostaglandin F2α (PGF2α) and endothelin-1 (ET-1): Is ET-1 a mediator of the luteolytic actions of PGF2α or a tonic inhibitor of progesterone secretion? Biol Reprod 2005;72:633–42. https://doi.org/10.1095/biolreprod.104.034736.

[46] Trevisol E, Mogollón García HD, Ackermann CL, Lacerda W, Pires RML, Laufer-Amorin R, et al. Partial luteolysis during early diestrus in cattle downregulates VEGFA expression and reduces large luteal cell and corpus luteum sizes and plasma progesterone concentration. Theriogenology 2020;158:188–95. https://doi.org/10.1016/j.theriogenology.2020.09.015.

[47] Korzekwa AJ, Lukasik K, Pilawski W, Piotrowska-Tomala KK, Jaroszewski JJ, Yoshioka S, et al. Influence of prostaglandin F2α analogues on the secretory function of bovine luteal cells and ovarian arterial contractility in vitro. Vet J 2014;199:131–7. https://doi.org/10.1016/j.tvjl.2013.09.021.

[48] Peluffo MC, Bussmann L, Stouffer RL, Tesone M. Expression of caspase-2, -3, -8 and -9 proteins and enzyme activity in the corpus luteum of the rat at diferent stages during the natural estrous cycle. Reproduction 2006;132:465–75. https://doi.org/10.1530/rep.1.00910.

[49] Maalouf SW, Liu WS, Pate JL. MicroRNA in ovarian function. Cell Tissue Res 2016;363:7–18. https://doi.org/10.1007/s00441-015-2307-4.

[50] Otsuka M, Zheng M, Hayashi M, Lee JD, Yoshino O, Lin S, et al. Impaired microRNA processing causes corpus luteum insufficiency and infertility in mice. J Clin Invest 2008;118:1944–54. https://doi.org/10.1172/JCI33680.

[51] Andreas E, Pandey HO, Hoelker M, Salilew-Wondim D, Gebremedhn S, Schellander K, et al. The regulatory role of miR-20a in bovine cumulus cells and its contribution to oocyte maturation. Zygote 2021. https://doi.org/10.1017/S0967199420000933.

[52] M Z, Q Z, Y H, L X, Y J, C Z, et al. miR-181a increases FoxO1 acetylation and promotes granulosa cell apoptosis via SIRT1 downregulation. Cell Death Dis 2017;8. https://doi.org/10.1038/CDDIS.2017.467.

[53] McBride D, Carré W, Sontakke SD, Hogg CO, Law A, Donadeu FX, et al. Identification of miRNAs associated with the follicular-luteal transition in the ruminant ovary. Reproduction 2012;144:221–33. https://doi.org/10.1530/REP-12-0025.

APPENDIX

Appendix 1. miRNA primers sequency.

miR ID	Primers sequence (5' - 3')
bta-miR-let-7a-3p	CTATACAATCTACTGTCTTTC
bta-miR-let-7b	TGAGGTAGTAGGTTGTGTGGTT
bta-miR-199-3p	ACAGTAGTCTGCACATTGGTTA
bta-miR-let-7e	TGAGGTAGGAGGTTGTATAGT
bta-miR-let-7g	TGAGGTAGTAGTTTGTACAGTT
bta-miR-10b	TACCCTGTAGAACCGAATTTGTG
bta-miR-125a	TCCCTGAGACCCTTTAACCTGTG
bta-miR-125b	TCCCTGAGACCCTAACTTGTGA
bta-miR-126-5p	CATTATTACTTTTGGTACGCG
bta-miR-132	TAACAGTCTACAGCCATGGTCG
bta-miR-142-3p	AGTGTTTCCTACTTTATGGATG
bta-miR-143	TGAGATGAAGCACTGTAGCTCG
bta-miR-145	GTCCAGTTTTCCCAGGAATCCCT
bta-miR-146a	TGAGAACTGAATTCCATAGGTTGT
bta-miR-15a	TAGCAGCACATAATGGTTTGT
bta-miR-17-5p	CAAAGTGCTTACAGTGCAGGTAGT
bta-miR-181a	AACATTCAACGCTGTCGGTGAGTT
bta-miR-182	TTTGGCAATGGTAGAACTCACACT
bta-miR-183	TATGGCACTGGTAGAATTCACTG
bta-miR-186	CAAAGAATTCTCCTTTTGGGCT
bta-miR-190a	TGATATGTTTGATATATTAGGT
bta-miR-21-5p	TAGCTTATCAGACTGATGTTGACT
bta-miR-202	TTCCTATGCATATACTTCTTT
bta-miR-20a	TAAAGTGCTTATAGTGCAGGTAG
bta-miR-210	ACTGTGCGTGTGACAGCGGCTGA
bta-miR-23a	ATCACATTGCCAGGGATTTCCA
bta-miR-26a	TTCAAGTAATCCAGGATAGGCT
bta-miR-29a	CTAGCACCATCTGAAATCGGTTA
bta-miR-30a-5p	TGTAAACATCCTCGACTGGAAGCT
bta-miR-320a	AAAAGCTGGGTTGAGAGGGCGA
bta-miR-33a	GTGCATTGTAGTTGCATTGCA
bta-miR-34a	TGGCAGTGTCTTAGCTGGTTGT
bta-miR-378	ACTGGACTTGGAGTCAGAAGGC
bta-miR-450a	TTTTGCGATGTGTTCCTAATAT
bta-miR-455-3p	GCAGTCCATGGGCATATACACT
bta-miR-503-3p	GGAGTATTGTTTCTGCTGCCCGG
bta-miR-7	TGGAAGACTAGTGATTTTGTTGTT
bta-miR-99a-3p	CAAGCTCGCTTCTATGGGT
bta-miR-92a	TATTGCACTTGTCCCGGCCTGT

Appendix 2. Immunohistochemistry slide proven with the aid of an optical scope (IX70, Olympus Corporation, Japan), using 40x magnification. Figure courtesy of Ana Clara Degan Matos, 2021.